

# **BEHAVIOR OF FLAT PLATES WITH LARGE OPENING IN COLUMN STRIP**

## **INTRODUCTION**

### **General**

A solid slab supported on beams on all four sides was the original slab system in reinforced concrete. As time progressed and technology evolved, the column-line beams gradually began to disappear. The resulting slab system consisting of solid slabs supported directly on columns is called the flat slab.

A flat plate floor is essentially a flat slab floor with the dropped panels and column capitals omitted, so that a floor of uniform thickness is carried directly by prismatic column. Flat plate floors have been found to be economical and otherwise advantageous for such uses as apartment buildings, where the spans are moderate and load relatively light. The construction depth for each floor is held to the absolute minimum, with resultant saving in overall height of the building. The smooth underside of the slab allowed for planning flexibility and facilitates the installation of infrastructures such as air ventilation, electricity or sanitary ducts. Minimum construction time and low labor costs result from the very simple formwork. In recent times it has been widely used for buildings such as shopping centers, office buildings, warehouses, hotels and schools.

In flat plate, shear stresses near the columns may be very high. The transfer of moments from slab to columns may further increase these shear stresses. In the case of flat plate that has an opening for drainage tubes, air ventilation ducts, loading machines or instruments, architectural works, etc., the size of opening is always large. The opening is more critical to the strength of flat plate when it is open in the area of column strip. The study of behavior of flat plate with large opening in column strip is necessary to solve these problems.

### **Statement of Problems**

The analysis of flat plate with opening is an inherent complicated problem. This problem is described by differential equations or by an integral expression. Either description may be used to formulate finite element. Finite element method (FEM) is a method for numerical solution. Finite element formulations, in ready-to-use form, are contained in general purpose FEM programs. This research used FEM program to solve this problem with software STAAD.Pro 2002.

## **Objectives**

1. To study the effect of location and size of the rectangular openings in column strips to the bending moments and shears of the flat plate.
2. To study the percentage of stress resultant change of the flat plate with openings.

## **Scope of Study**

This research attempts to study behavior of flat plate with large opening in column strip.

1. The flat plate models are nine square panels comprising of three by three equal width panels supported by sixteen square columns.
2. Load on flat plat is uniform distributed load.
3. The thickness of flat plate follows E.I.T. standard.
4. The shape of opening is rectangular with varied size.
5. Use elastic plate theory and flat plate is homogeneous material.

## LITERATURE REVIEW

The Engineering Institute of Thailand (E.I.T) standard (1973) defined flat plate and their components as follows:

Flat plate is concrete slab that is reinforced in two direction or more and absence of beams along the interior column lines, but edge beams may or may not be used at the exterior edges of the floor. For analysis, the slab system is divided into design strips consisting of a column strip and half middle strip

The column strip is design strips with a width on each side of a column centerline equal to one-quarter the transverse or longitudinal span, whichever is smaller. The middle strip is a design strip bounded by two column strips.

The criteria for the opening in flat plate are as follow.

1. Openings of any size shall be permitted in the area common to intersecting middle strips, provided total amount of reinforcement required for the panel without the opening is maintained.

2. In the area common to intersecting column strips, not more than one-eighth the width of column strip in either span shall be interrupted by openings. An amount of reinforcement equivalent to that interrupted by an opening shall be added on the sides of the opening.

3. In the area common to one column strip and one middle strip, not more than one-quarter of the reinforcement in either strip shall be interrupted by openings. An amount of reinforcement equivalent to that interrupted by an opening shall be added on the sides of the opening.

4. Openings of any size shall be permitted in slab systems if shown by analysis that the design strength is at least equal to the required strength.

When openings in slabs are located at a distance less than ten times the slab thickness from a concentrated load or reaction area, the critical perimeter must be reduced as shown in Figure 1.

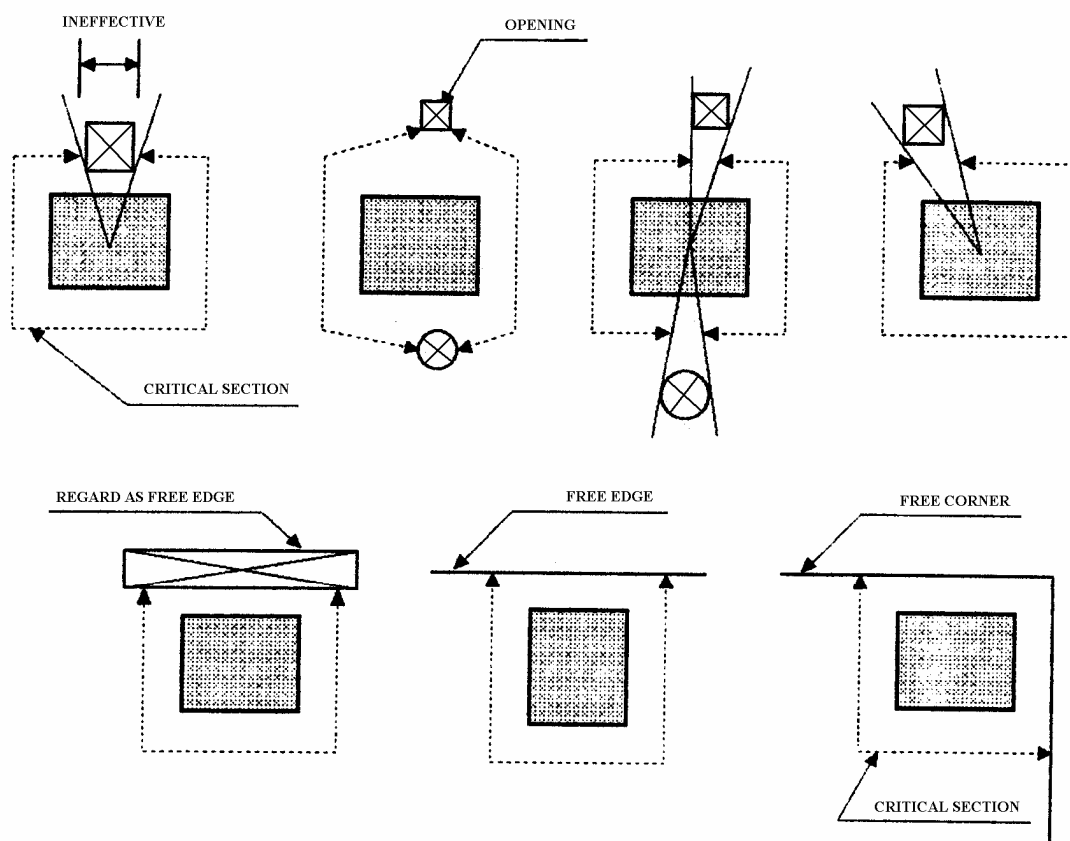


**Figure 1** Critical perimeter for shear

Source: E.I.T Standard (1973)

The Building Code Requirements for Structural Concrete (ACI 318M-95) (1995) defined the criteria of opening in slab system as follows:

1. Openings of any size shall be permitted in slab systems if shown by analysis that the design strength is at least equal to the required strength considering required strength and design strength, and that all serviceability conditions, including the specified limits on deflections, are met.

2. As an alternative to special analysis as required by article 1, openings shall be permitted in slab systems without beam only in accordance with the following:

2.1 Openings of any size shall be permitted in the area common to intersecting middle strips, provided total amount of reinforcement required for the panel without the opening is maintained.

2.2 In the area common to intersecting column strips, not more than one-eighth the width of column strip in either span shall be interrupted by openings. An amount of reinforcement equivalent to that interrupted by an opening shall be added on the sides of the opening.

2.3 In the area common to one column strip and one middle strip, not more than one-quarter of the reinforcement in either strip shall be interrupted by openings. An amount of reinforcement equivalent to that interrupted by an opening shall be added on the sides of the opening.

2.4 Shear requirements of openings in slabs shall be satisfied.

3. When openings in slabs are located at a distance less than ten times the slab thickness from a concentrated load or reaction area, or when openings in flat slabs are located within column strips, the critical slab sections for shear shall be modified as follows:

3.1 For slabs without shearheads, that part of the perimeter of the critical section that is enclosed by straight lines projecting from the centroid of the column, concentrated load, or reaction area and tangent to the boundaries of the openings shall be considered ineffective.

3.2 For slabs with shearheads, the ineffective portion of the perimeter shall be one-half of that defined in article 3.1.

3.3 The locations of the effective portion of the critical section near typical openings and free edges are shown by dash line in Figure 2.

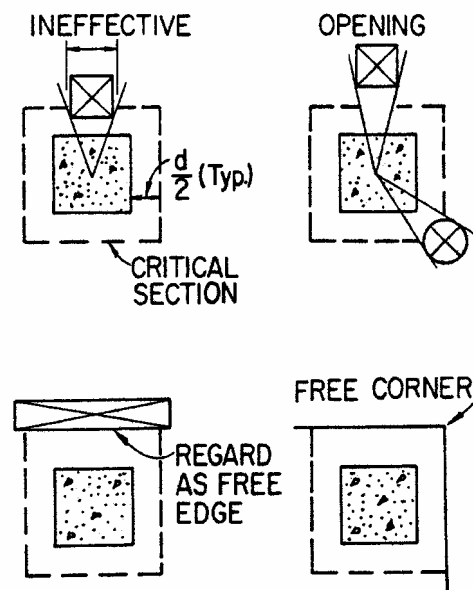


**Figure 2** Critical perimeter for shear  
Source: ACI 318M-95 (1995)

Salakawy *et.al.* (1998) studied the punching shear in flat slabs with opening by using shear stud in flat slab to increase the shear strength of the slab. The punching shear was according to the concentrate load and moment transfer analysis by finite element method. The slab model is  $1540 \times 1020 \times 120$  mm connected with square column size 250 mm divided into two types using six examples of slab without shear stud and four examples of slab with shear stud. The results of testing shear stud increase shear strength of slab and increase ductility of connection between slab and column.

Prawat (2000) studied the behavior of flat plates with openings of any size, varying from the size permitted by the building code and standard of ACI and EIT to the size larger than permitted size. The four locations of openings were the openings in the area common to intersecting middle strips, the area common to one column strip and one middle strip, the area common to one middle-column strip and one middle strip and the area common to intersecting column strips. The flat plate models were nine square panels comprised of three by three equal width panels supported by sixteen square columns. These plate models with varied square opening size subjected to uniform distributed loads were analyzed and investigated for maximum bending moment, shear force and deflections by used finite element software program.

The result of study indicated that the openings in the area common to the intersecting middle strips could be any size according to the code. In the area common to one column strip and one middle strip, the bending moments and shears were increased if the opening size was larger than the permitted one. These increasing values were considered to be safe for the plate if the total amount of reinforcement was still maintained. This result was also applied to the plates with opening in the area common to one middle-column strip and one middle strip. For the opening in the area common to intersecting column strips, no significant changes in behavior of plate were found if the opening size was according to the code. The additional reinforcement required by the code was required on the sides and corner of the opening. If the opening size was larger than the specified by the code, the bending moments and shears were increased by varying amount according to its size and location closing to the column.

## Theoretical Methods

Plate means a flat body whose thickness is much smaller than its other dimensions. Plate theory can be divided into two theories. The first is called thin-plate theory or Kirchhoff theory, which prohibits transverse shear deformation, in recognition of Kirchhoff's research on plate theory 1850. The second is usually known as Mindlin theory, which accounts transverse shear deformation. Either of two theories provide a mathematical model that can be solved by finite element analysis (FEA), using appropriately formulate plate elements.

### Notation

Figure 3a, represent slopes of the plate surfaces  $w_{,x}$  and  $w_{,y}$  by the right hand rule which produces arrows that point in the negative  $y$  and positive  $x$  directions respectively. The slope of the plate surface  $w_{,x}$  and  $w_{,y}$  are replaced by  $\psi_x$  and  $\psi_y$  respectively as shown in Figure 3b that represent the rotations of a midsurface of plates.

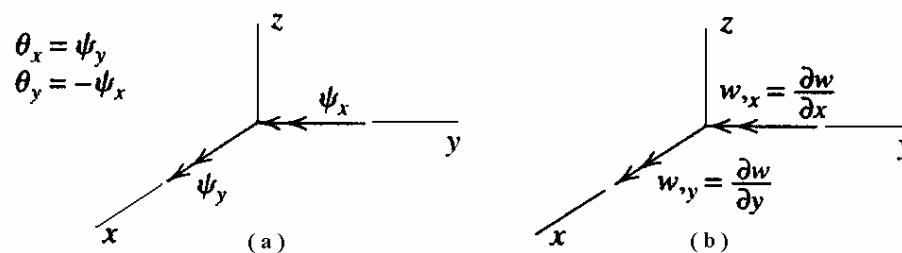


**Figure 3** Notation for rotation components of a midsurface-normal and Slope of a plate surface

Source: Cook *et.al.* (2002)

### Plate Theory

A plate of thickness  $t$  has a midsurface at distance  $t/2$  from each lateral surface. For analysis, locate the  $xy$  plane in the plate midsurface as shown in Figure 4 where  $z = 0$  identifies the midsurface. The bending of homogeneous plate makes the midsurface a neutral surface, that is  $\varepsilon_x = \varepsilon_y = \gamma_{xy} = 0$  at  $z = 0$ .

The line that is straight and normal to the midsurface before load is applied remains straight but not necessarily normal to the deformed midsurface. Rotation of this straight line has components  $\psi_x$  and  $\psi_y$ . A point not on the midsurface has the  $x$ -direction displacement  $u$  shown in Figure 5. A similar cross section, viewed in the negative  $x$ -direction, provides  $y$ -direction displacement  $v$ . Hence, for small displacements and rotations, strains can be written as

$$\begin{aligned}
 u &= -z\psi_x \\
 v &= -z\psi_y \\
 \varepsilon_x &= -z\psi_{x,x} \\
 \varepsilon_y &= -z\psi_{y,y} \\
 \gamma_{xy} &= -z(\psi_{x,y} + \psi_{y,x}) \\
 \gamma_{yz} &= w_{,y} - \psi_y \\
 \gamma_{zx} &= w_{,x} - \psi_x
 \end{aligned} \tag{1}$$

where comma denotes differentiation with respect to the following subscript and  $w$  is the lateral ( $z$ -direction) deflection of the midsurface.

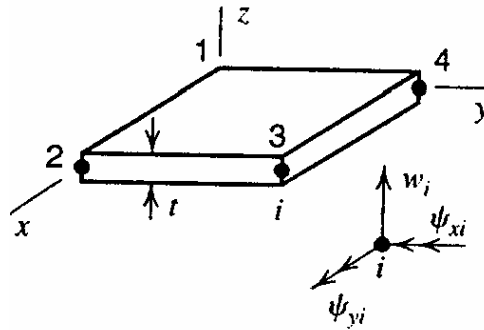


**Figure 4** A plate element with corner nodes, showing typical nodal d.o.f.  
Source: Cook *et.al.* (2002)

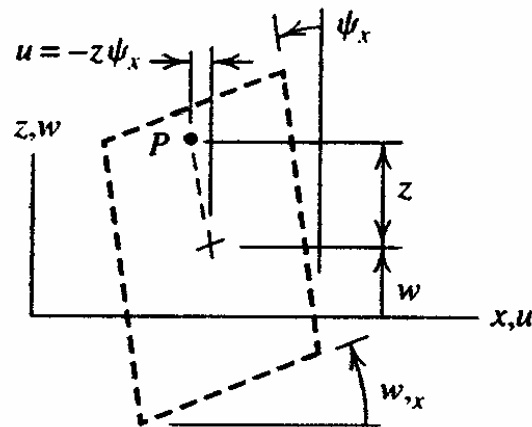


**Figure 5** A deformed plate cross section, view in the + y direction.

Thickness- direction is assumed to remain straight

Source: Cook *et.al.* (2002)

Equations 1 are the basis of Mindlin plate theory. In Kirchhoff plate theory, a straight line normal to the undeformed midsurface is assumed to remain straight and normal to the deformed midsurface. Thus  $w_{,x} = \psi_y$  and  $w_{,y} = \psi_x$  and transverse shear deformation is zero throughout a Kirchhoff plate. Many practical plates can be regarded as Kirchhoff plates because they are thin enough for transverse shear deformation to be negligible.

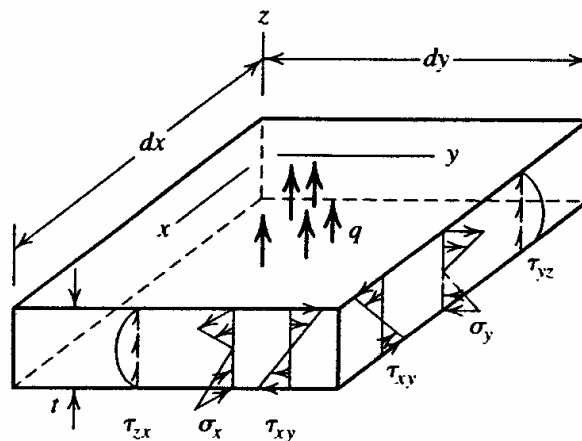


**Figure 6** Stresses and distributed lateral force  $q$  on a differential element of plate

Source: Cook *et.al.* (2002)

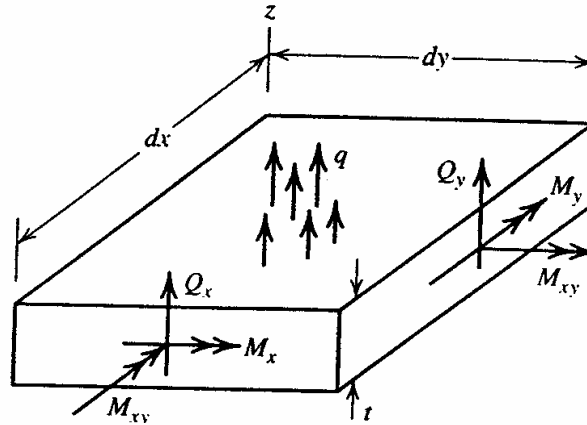


**Figure 7** Moment and transverse shear forces associated with stresses  
Source: Cook *et.al.* (2002)

Stresses on cross sections are depicted in Figure 6. It is customary to associate these stresses with moments and force per unit length in the  $xy$  plane which are depicted in Figure 7. Thus

$$\begin{aligned} M_x &= \int_{-t/2}^{t/2} \sigma_x z \, dz \\ M_y &= \int_{-t/2}^{t/2} \sigma_y z \, dz \\ M_{xy} &= \int_{-t/2}^{t/2} \tau_{xy} z \, dz \end{aligned} \quad (2)$$

$$\begin{aligned} Q_x &= \int_{-t/2}^{t/2} \tau_{zx} \, dz \\ Q_y &= \int_{-t/2}^{t/2} \tau_{yz} \, dz \end{aligned} \quad (3)$$

Customarily, normal stress  $\sigma_z$  is considered negligible in comparison with  $\sigma_x$ ,  $\sigma_y$ , and  $\tau_{xy}$ . Then, for a linear elastic and isotropic material, the stress-strain relation in each  $z$ -parallel layer of the plate is the familiar plane-stress expression

$$\begin{Bmatrix} \sigma_x \\ \sigma_y \\ \tau_{xy} \end{Bmatrix} = \frac{E}{1-\nu^2} \begin{bmatrix} 1 & \nu & 0 \\ \nu & 1 & 0 \\ 0 & 0 & \frac{1-\nu}{2} \end{bmatrix} \begin{pmatrix} \begin{Bmatrix} \varepsilon_x \\ \varepsilon_y \end{Bmatrix} - \begin{Bmatrix} \varepsilon_{x_0} \\ \varepsilon_{y_0} \end{Bmatrix} \\ \gamma_{xy} \\ 0 \end{pmatrix} \quad (4)$$

where  $\varepsilon_{x_0}$  and  $\varepsilon_{y_0}$  are initial strains.

### Kirchhoff Plate Theory

Transverse shear deformation is prohibited,  $w_{,x} = \psi_x$  and  $w_{,y} = \psi_y$  hence  $\varepsilon_x = -z w_{,xx}$ ,  $\varepsilon_y = -z w_{,yy}$ , and  $\gamma_{xy} = -2z w_{,xy}$ . These strain-curvature relations may be substituted into equation 4 and the resulting expressions for stress into equation 3, 4. Thus the moment-curvature relations for a homogeneous and isotropic Kirchhoff plate are

$$\{M\} = -[D](\{\kappa\} - \{\kappa_0\}) \quad (5)$$

or

$$\begin{Bmatrix} M_x \\ M_y \\ M_{xy} \end{Bmatrix} = - \begin{bmatrix} D & \nu D & 0 \\ \nu D & D & 0 \\ 0 & 0 & \frac{(1-\nu)D}{2} \end{bmatrix} \left( \begin{Bmatrix} w_{,xx} \\ w_{,yy} \\ 2w_{,xy} \end{Bmatrix} - \{\kappa_0\} \right) \quad (6)$$

where  $D = \frac{E t^3}{12(1-\nu^2)}$  is called flexural rigidity.

$\{\kappa_0\} = [2\alpha T_0/t \quad 2\alpha T_0/t \quad 0]^T$  is initial curvature, let temperature vary linearly with  $z$  from  $T_0$  at  $z = -t/2$  to  $-T_0$  at  $z = t/2$

### Mindlin Plate Theory

Three fields  $w$ ,  $\psi_x$ , and  $\psi_y$  are expressed in terms of  $x$  and  $y$  in order to describe the state of deformation and stress throughout the Mindlin plate. For homogeneous, isotropic, and linear elastic material, relation is analogous to Eqs.6 but for Mindlin plate are

$$\begin{Bmatrix} M_x \\ M_y \\ M_{xy} \\ Q_x \\ Q_y \end{Bmatrix} = - \begin{bmatrix} & & 0 & 0 \\ & [D] & 0 & 0 \\ & & 0 & 0 \\ 0 & 0 & 0 & kGt & 0 \\ 0 & 0 & 0 & 0 & kGt \end{bmatrix} \left( \begin{Bmatrix} \psi_{x,x} \\ \psi_{y,y} \\ \psi_{x,y} + \psi_{y,x} \\ \psi_x - w_{,x} \\ \psi_y - w_{,y} \end{Bmatrix} - \{\kappa_0\} \right) \quad (7)$$

Where  $[D]$  is the same square matrix in Eq.5. Factor  $k$  accounts for the effect of transverse shear stress, and  $kt$  can be regarded as the effective thickness for transverse shear deformation. The value of  $k$  for homogeneous plate is  $k = 5/6$ .

### Formulation Techniques

Most plates are thin enough for transverse shear deformation to be negligible. Therefore, a plate problem is solved when lateral deflection  $w = w(x, y)$  of the midsurface has been determined. Plate element were 12 degree of freedom (d.o.f.) rectangle, with a node at each corner and three d.o.f. per node.

$$w = \begin{bmatrix} 1 & x & y & x^2 & xy & y^2 & x^3 & x^2y & xy^2 & y^3 & x^3y & xy^3 \end{bmatrix} \{a\} \quad (8)$$

where the twelve  $a_i$  in  $\{a\}$  are generalized d.o.f.

Define the displacement over an element by shape function interpolation from nodal d.o.f.  $\{d\}$ .

$$w = [N] \{d\} \quad (9)$$

Where  $[N]$  is shape function

$$[N] = [N_1 \quad N_2 \quad N_3 \quad \cdots \quad N_{12}] \quad (10)$$

$$\{d\} = [w_1 \quad \theta_{x1} \quad \theta_{y1} \quad w_2 \quad \theta_{x2} \quad \theta_{y2} \quad \cdots \quad w_4 \quad \theta_{x4} \quad \theta_{y4}]^T \quad (11)$$

A linear elastic material, without initial stress or strain, the strain energy  $U$  can be expressed by

$$U = \int \frac{1}{2} \{\varepsilon\}^T [E] \{\varepsilon\} dV \quad (12)$$

Strain energy  $U$  in the plate due to nodal displacements can be expressed in terms of curvature  $\{\kappa\}$  by setting  $\gamma_{yz} = \gamma_{zx} = 0$  in Eqs.1.

$$\{\kappa\} = \begin{Bmatrix} w_{,xx} \\ w_{,yy} \\ 2w_{,xy} \end{Bmatrix} = [B] \{d\} \quad (13)$$

where

$$[B] = \begin{Bmatrix} \frac{\partial^2}{\partial x^2} \\ \frac{\partial^2}{\partial y^2} \\ \frac{\partial^2}{\partial x \partial y} \end{Bmatrix} [N] \quad (14)$$

Then Eq.12 becomes

$$U = \int \frac{1}{2} \{\kappa\}^T [D] \{\kappa\} dA \quad (15)$$

where  $A$  is the midsurface area and  $[D]$  is given by Eq.5 for a homogeneous and isotropic plate.

Hence, with integration confined to a single element, Eq.15 provides the element strain energy and element stiffness matrix  $[k]$ .

$$U = \frac{1}{2} \{d\}^T [k] \{d\} \quad (16)$$

where

$$[k] = \int [B]^T [D] [B] dA \quad (17)$$

The potential of applied loads  $\Omega$  can be expressed by

$$\Omega = \int \{\bar{d}\}^T \{q(x, y)\} dA \quad (18)$$

where

$$\{q(x, y)\} = [F_{z1} \quad M_{x1} \quad M_{y1} \quad \cdots \quad F_{z4} \quad M_{x4} \quad M_{y4}]^T \quad (19)$$

$$\{\bar{d}\} = \{d\} [N]^T \quad (20)$$

The potential energy  $\Pi$  can be expressed by

$$\Pi = U + \Omega \quad (21)$$

Substitute Eqs.16 and 18 into Eq.21 then

$$\Pi = \frac{1}{2} \{d\}^T [k] \{d\} - \int \{\bar{d}\}^T \{q(x, y)\} dA \quad (22)$$

Applying the principle of stationary potential energy  $\frac{\partial \Pi}{\partial \{d\}} = 0$ , then Eq.22 become

$$[k] \{d\} = \{p\} \quad (23)$$

where

$$\{p\} = \int [N]^T dA \quad (24)$$

The equilibrium equation in Eq.23 is for single element, then for whole structure the equilibrium equation can be expressed by

$$[K] \{u\} = \{F\} \quad (25)$$

### **STAAD.Pro 2002 Finite Element Formulation**

In program STAAD.Pro 2002, the plate finite element is based on the hybrid element formulation. The element can be 3-node (triangular) or 4-node (quadrilateral). The thickness of the element may be different from one node to another. A complete quadratic stress distribution is assumed. For plane stress action as shown in Figure 8, the assumed stress distribution is as follows.

$$\begin{pmatrix} \sigma_x \\ \sigma_y \\ \tau_{xy} \end{pmatrix} = \begin{bmatrix} 1 & x & y & 0 & 0 & 0 & 0 & x^2 & 2xy & 0 \\ 0 & 0 & 0 & 1 & x & y & 0 & y^2 & 0 & 2xy \\ 0 & -y & 0 & 0 & 0 & -x & 1 & -2xy & -y^2 & -x^2 \end{bmatrix} \begin{pmatrix} a_1 \\ a_2 \\ a_3 \\ \vdots \\ a_{10} \end{pmatrix} \quad (26)$$

Where  $a_1$  through  $a_{10}$  is constant of stress polynomials.

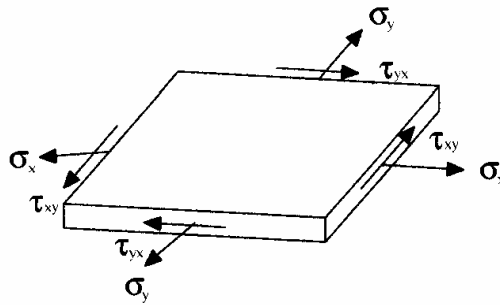


**Figure 8** Plane stress action

Source: Research Engineers, Intl. (2002)

The following quadratic stress distribution is assumed for plate bending action as shown in Figure 9.

$$\begin{pmatrix} M_x \\ M_y \\ M_{xy} \\ Q_x \\ Q_y \end{pmatrix} = \begin{bmatrix} 1 & x & y & 0 & 0 & 0 & 0 & 0 & 0 & x^2 & xy & 0 & 0 \\ 0 & 0 & 0 & 1 & x & y & 0 & 0 & 0 & 0 & 0 & xy & y^2 \\ 0 & 0 & 0 & 0 & 0 & 0 & 1 & x & y & -xy & 0 & 0 & -xy \\ 0 & 1 & 0 & 0 & 0 & 0 & 0 & 0 & 1 & x & y & 0 & -x \\ 0 & 0 & 0 & 0 & 0 & 1 & 0 & 1 & 0 & -y & 0 & x & y \end{bmatrix} \begin{pmatrix} a_1 \\ a_2 \\ a_3 \\ \vdots \\ \vdots \\ a_{13} \end{pmatrix} \quad (27)$$

Where  $a_1$  through  $a_{10}$  is constant of stress polynomials.

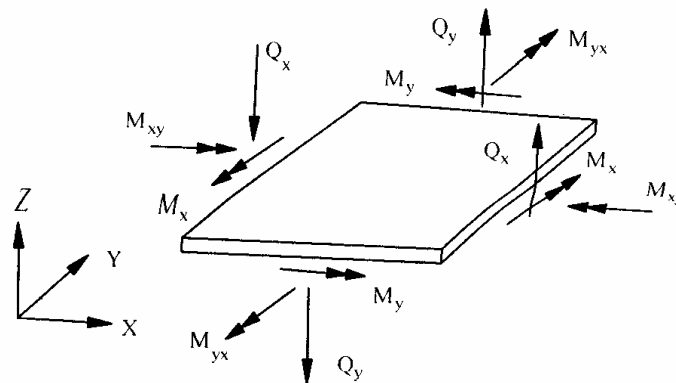


**Figure 9** Plate bending action

Source: Research Engineers, Intl. (2002)

The distinguishing features of this finite element are

1) Displacement compatibility between the plane stress component of one element and the plate bending component of an adjacent element which is at an angle to the first (Figure 10) is achieved by the elements. This compatibility requirement is usually ignored in most flat plate elements.

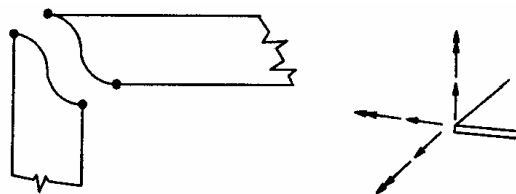


**Figure 10** Displacement compatibility

Source: Research Engineers, Intl. (2002)

2) The out of plane rotational stiffness from the plane stress portion of each element is usefully incorporated and not treated as a dummy as is usually done in most commonly available commercial software.

3) Despite the incorporation of the rotational stiffness mentioned previously, the elements satisfy the patch test absolutely.

4) These elements are available as triangles and quadrilaterals, with corner nodes only, with each node having six degrees of freedom.

5) These elements are the simplest forms of the flat plate elements possible with corner nodes only and six degrees of freedom per node. Yet solutions to sample problems converge rapidly to accurate answers even with the large mesh size.

6) These elements may be connected to plane/space frame members with full displacement compatibility. No additional restraints/releases are required.

7) Out of plane shear strain energy is incorporated in the formulation of the plate bending component. As a result, the elements respond to Poisson boundary conditions which are considered to be more accurate than the customary Kirchhoff boundary conditions.

8) The plate bending portion can handle thick and thin plates, thus extending the usefulness of the plate elements into a multiplicity of problems. In addition, the thickness of the plate is taken into consideration in calculating the out of plane shear.

9) The plane stress triangle behaves almost on par with the well known linear stress triangle. The triangles of most similar flat elements incorporate the constant stress triangle which has very slow rates of convergence.

10) Stress retrieval at nodes and at any point within the element.

The precise orientation of local coordinates is determined as follows (Figure 11).

1) Designate the midpoints of the four or three element edges IJ, JK, KL, LI by M, N, O, P respectively.

2) The vector pointing from P to N is defined to be the local x-axis (In a triangle, this is always parallel to IJ).

3) The cross-product of vectors PN and MO (for a triangle, ON and MK) defines the local z-axis, i.e.,  $z = \text{PN} \times \text{MO}$ .

4) The cross product of vectors z and x defines the local y-axis, i.e.,  $y = z \times x$ .

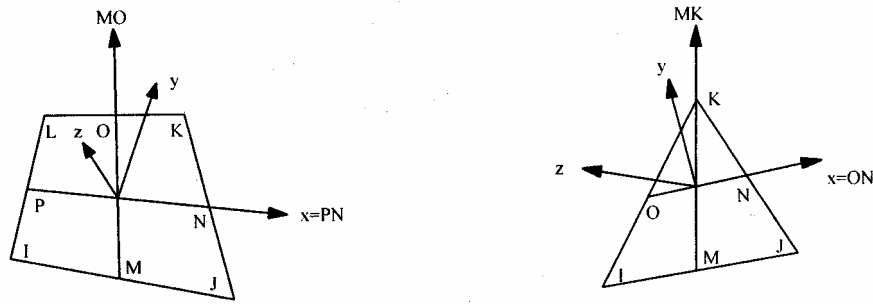


**Figure 11** Element local coordinate system  
 Source: Research Engineers, Intl. (2002)

The sign convention of output force and moment resultants is illustrated in Fig.12. All element stress output is in the local coordinate system. Following are the items included in the element stress output.

- |                    |   |
|--------------------|---|
| $SQ_x, SQ_y$       | Shear stresses (Force/unit length/thickness)      |
| $S_x, S_y, S_{xy}$ | Membrane stresses (Force/unit length/thickness)   |
| $M_x, M_y, M_{xy}$ | Bending moment per unit width (Force/unit length) |
| $S_{max}, S_{min}$ | Principal stresses (Force/unit area)              |

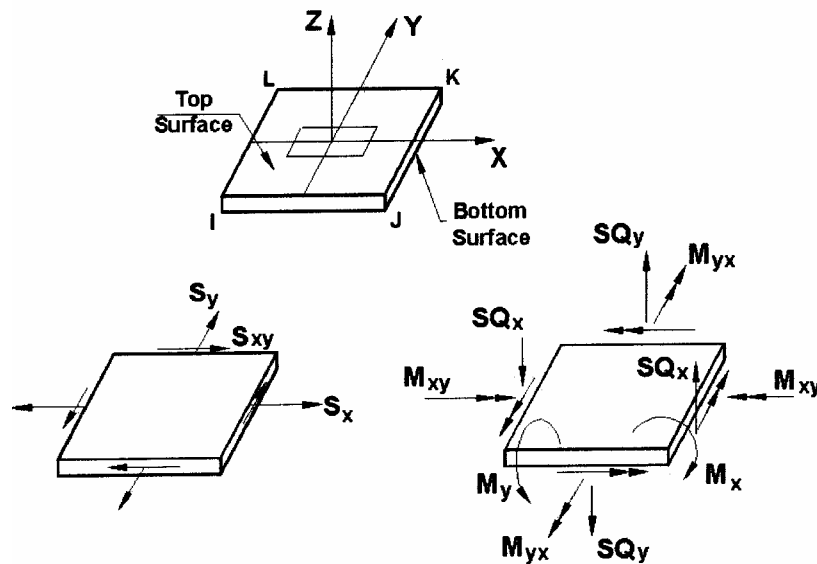


**Figure 12** Sign convention of element forces  
 Source: Research Engineers, Intl. (2002)

## MATERIALS AND METHODS

### Materials

1. PC-Computer with CPU speed 1.6 GHz and 256 Mbytes RAMS
2. Software STAAD.*Pro* 2002

### Methods

The methods to study behavior of flat plate with opening in the area of column strip are as follows:

#### 1. Verify Computer Program Testing

Before analyzing the flat plate, the software STAAD.*Pro* 2002 was tested on sample structure. The samples used were rectangular slab on simply support and fixed support subjected to the uniform load. Compare the stress resultants between Levy's method and software STAAD.*Pro* 2002.

#### 2. Determine Critical Locations of Openings

Analyze the flat plates where openings are in the area common to intersecting column strips of flat plate. Determine the critical location of the openings in area of column strip by comparing the stress resultants between each other location.

#### 3. Determine Effect of Opening Size and Location on Stress Resultant Change

3.1 Analyze the flat plates with openings at the areas of critical locations by varying the size of openings at one-tenth, one-fifth, three-tenth, and two-fifth of the width of column strip. The size openings are varying in both direction of the plane of plate ( $x$  and  $y$  axes). Determine the relationship between the size of openings and percentage of stress resultants change in flat plate at column strip.

3.2 Analyze the flat plates with openings adjacent to all interior columns and all edge columns. Use the critical size of openings and determine the stress resultants change in flat plate.

## RESULTS AND DISCUSSION

### 1. Computer Program Testing

Analyze the rectangular slabs on simply support and fixed support as shown in Figure 13 that is subjected to the uniform load. Compare the stress resultants between Levy's method and software *STAAD.Pro 2002*.

Data of rectangular slab for analysis are as follows:

Size of slab	6.00 × 9.00	m
Thickness	0.20	m
Young's modulus	2.1E9	kg/m <sup>2</sup>
Uniform load	500	kg/m <sup>2</sup>
Poisson's ratio	0.3	

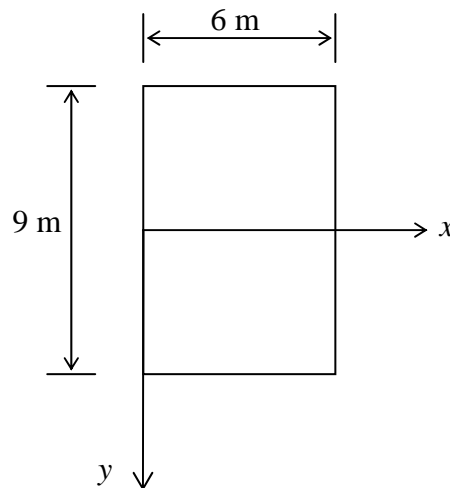


**Figure 13** Plan of rectangular slab on simple support and fixed support

1.1 Compare the stress resultants of rectangular slab that are subjected to uniform load. Boundary of slab is simply support as shown in Figure 14. Analyze the slab by program *STAAD.Pro 2002* and discrete the slab into the mesh of  $12 \times 18$  element. The size of element is  $0.5 \text{ m} \times 0.5 \text{ m}$ .

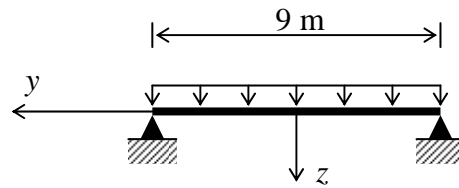


**Figure 14** Cross section of rectangular slab on simple support

**Table 1** Comparison of stress resultants of slab on simply support that are subjected to uniform load between Levy's method and program *STAAD.Pro 2002*

Coordinate (m)		$w$ (cm)		$M_x$ (kg-m)		$M_y$ (kg-m)		$Q_x$ (kg)		$Q_y$ (kg)	
x	y	S.Pro	Levy	S.Pro	Levy	S.Pro	Levy	S.Pro	Levy	S.Pro	Levy
3	0	0.324	0.325	1435	1462	881	896	1246	1272	1068	1089
% error		-0.3		-1.8		-1.6		-2.0		-1.9	

Source: Timoshenko (1959)

In Table 1, the deflection and stress resultants of Levy's method at the center of slab is greater than all *STAAD.Pro 2002* program results. The percentage error of deflection  $w$  is -0.3%. For percentage error of bending moment  $M_x$ ,  $M_y$ , and shear force  $Q_x$ ,  $Q_y$  are -1.8%, -1.6% and 2.0%, 1.9% respectively.

1.2 Compare the stress resultants of rectangular slab that are subjected to uniform load. Boundary of slab is fixed support as shown in Figure 15. Analyze the slab by program *STAAD.Pro 2002* and discrete the slab into the mesh of  $12 \times 18$  element. The size of element is  $0.5 \text{ m} \times 0.5 \text{ m}$ .

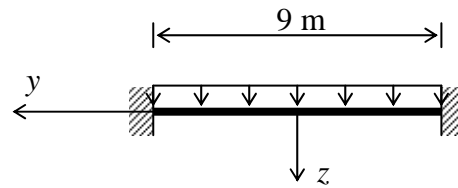


**Figure 15** Cross section of rectangular slab on fixed support

**Table 2** Comparison of stress resultants of slab on fixed support that are subjected to uniform load between Levy's method and program *STAAD.Pro 2002*

Coordinate (m)		$w$ (cm)		$M_x$ (kg-m)		$M_y$ (kg-m)		% error		
x	y	<i>S.Pro</i>	Levy	<i>S.Pro</i>	Levy	<i>S.Pro</i>	Levy	$w$	$M_x$	$M_y$
3	0	0.093	0.092	644	662	357	365	1	-2.7	-2.1
0	0	-	-	1321	1362	-	-	-	-3.0	-
3	4.5	-	-	-	-	1001	1026	-	-	-2.4

Source: Timoshenko (1959)

In Table 2, deflection and stress resultant of Levy method is greater than all *STAAD.Pro 2002* program results. The percentage error of deflection  $w$  is 1.0%. For bending moment  $M_x$ , and  $M_y$ , at center of slab are -2.7%, and -2.1% respectively. The percentage error of bending moment  $M_x$ , and  $M_y$  at fixed support are -3.0% and -2.4% respectively.

The percentage error of stress resultants from analysis of the rectangular slab by using *STAAD.Pro 2002* program compared to Levy's method as shown in Table 1 and 2 is less than 5%. This error is less than the error of approximate design of continuous plates with equal spans (Timoshenko, 1959) that use the error at 10%. It is noted that this program can be used to analyze the flat plate later.

## 2. Critical Locations of Openings

Analyze the flat plate as shown in Figure 16. The openings located in the area common to intersecting column strips of flat plate are as shown in Figure 17. The dimensions of the opening used equal the size of the column. Determine the critical location of the openings in area of column strip by comparing the stress resultants between each other location.

The data of flat plate for analysis are as follows:

Span	8	m
Thickness	0.25	m
Square column width	0.80	m
Uniform load	1450	kg/m <sup>2</sup>
Concrete; E	21.72E6	kN/m <sup>2</sup>
$\nu$	0.17	

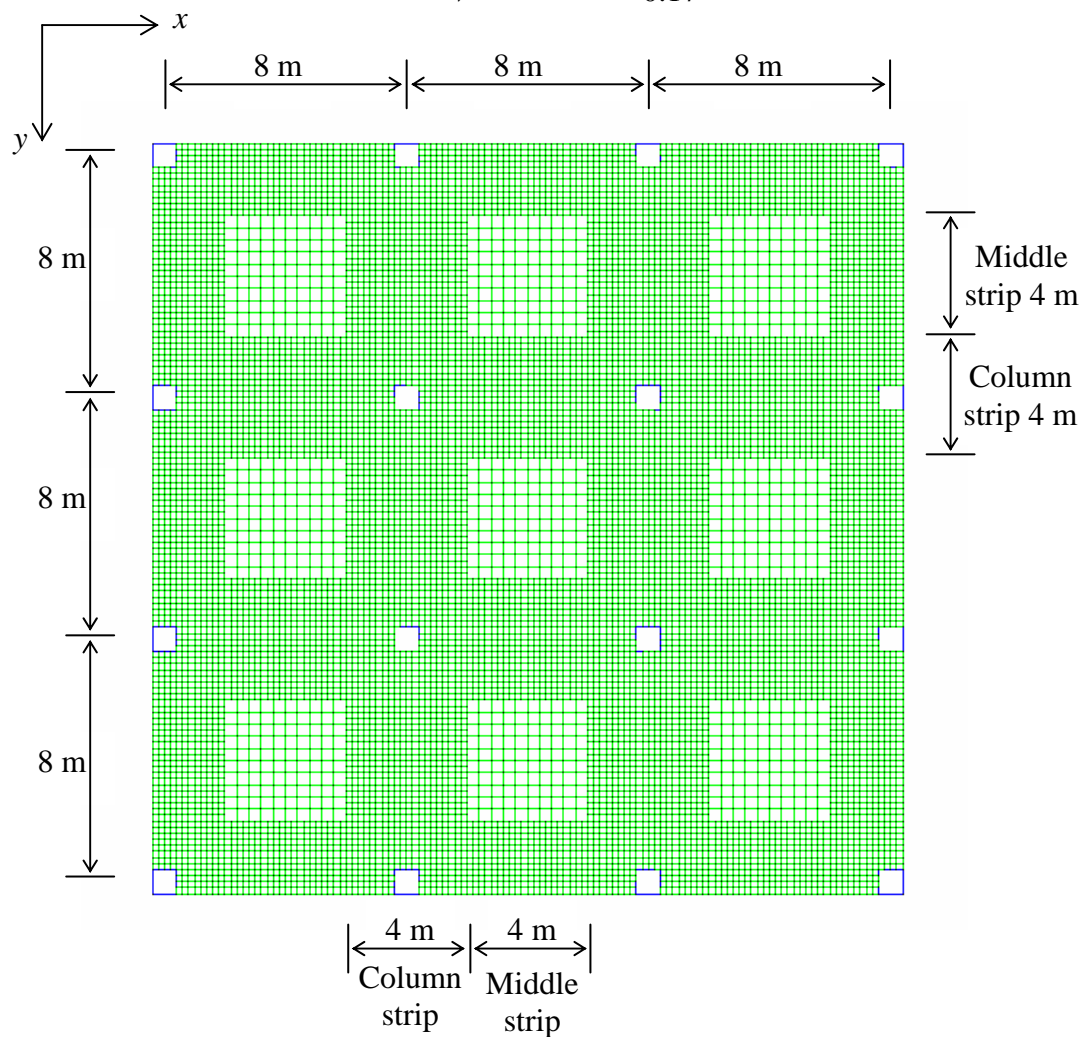


**Figure 16** Plan of flat plate (without opening)

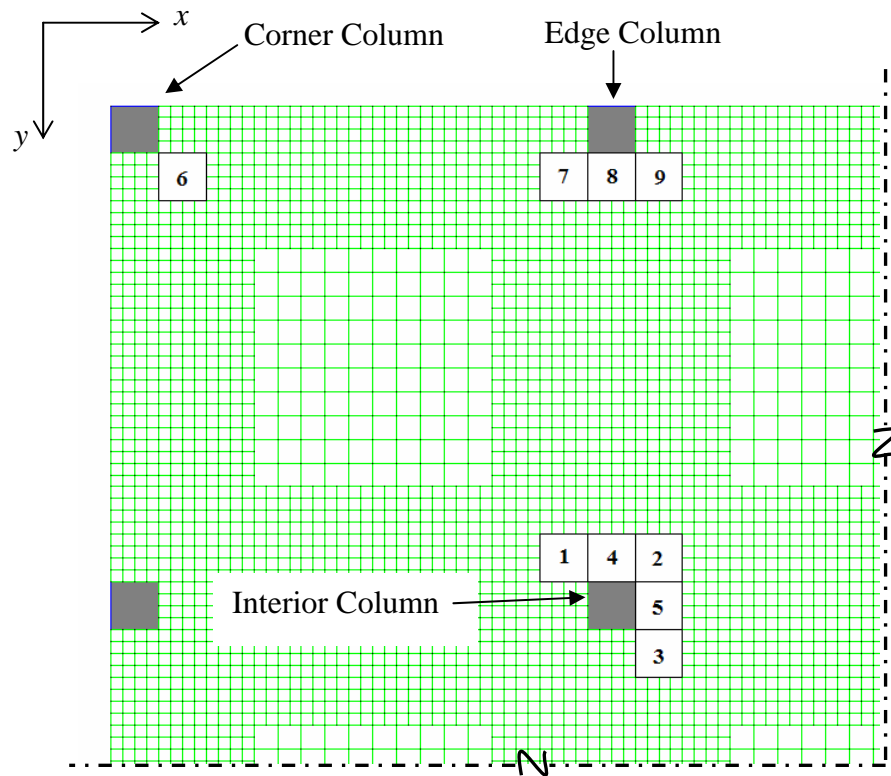


**Figure 17** Nine locations of openings in the area of column strip

**Table 3** Percentage of maximum stress resultants change of flat plate with opening in each location compared to flat plate without opening

Location of Opening	Percentage of Maximum Stress Resultants Change (%)			
	$Q_x$	$Q_y$	$M_x$	$M_y$
1	3.48	3.48	6.78	6.78
2	1.49	2.48	0.71	11.21
3	0.49	0.49	4.57	4.57
4	8.10	34.82	12.90	-0.46
5	20.87	22.67	8.29	17.05
6	26.96	26.96	-2.09	-2.09
7	-5.97	6.46	-11.74	-12.46
8	-8.71	8.80	-33.80	-23.42
9	-5.99	10.44	-10.99	-12.09

The openings in the area common to intersecting column strips of flat plate as shown in Figure 17 were classified into three categories. The first category consisted of openings close to the interior column were opening number 1 to 5. The next category was opening number 6 close to the corner column. And the last category was openings that close to the edge column were opening number 7 to 9. The dimension of the opening used equal to the size of the column is  $0.8\text{ m} \times 0.8\text{ m}$ . The percentage of maximum stress resultants change of flat plate with opening in each location compared to flat plate without opening is shown in Table 3.

First, consider the openings close to the interior column. The maximum percentage of shear stress change of flat plate at opening number 4 is 34.82% while percentage of bending moment change is 12.90%. The maximum percentage of bending moment change of flat plate at opening number 5 is 17.05% while percentage of shear stress change is 22.67%. Both openings number 4 and 5 are located at the face of the column. It shows that the openings at the face of column are critical location when compared with openings at corner of column, openings number 1, 2, and 3.

Next, consider the opening close to the corner column as the opening number 6. At this location the percentage of shear stress change is 26.96% which is greater than the openings close to the interior column while percentage of bending moment change is -2.09%.

Lastly, consider the openings close to the edge column as the opening number 7, 8, and 9. The maximum percentage of shear stress change of flat plate is opening number 9 at 10.44% while percentage of bending moment change is -12.09%. However, the percentage of shear stress change when opening at number 8 is 8.80% close to the opening number 9. The opening at number 8, the percentage of bending moment change is maximum equal to -33.80%. As the openings close to the interior column, the critical location of opening is located at the face of the column.

From the openings in three categories, the location of maximum bending moment is close to the face of column. For the location of maximum shear, it is close to the edge of opening or the face of column. The location of maximum stress resultant can be shown in Figure 18 to 26. It is shown that the openings at the face of the column are critical location. Even though the opening number 6 at the corner column gives the maximum percentage of shear stress change, in practice it is not open in this location.

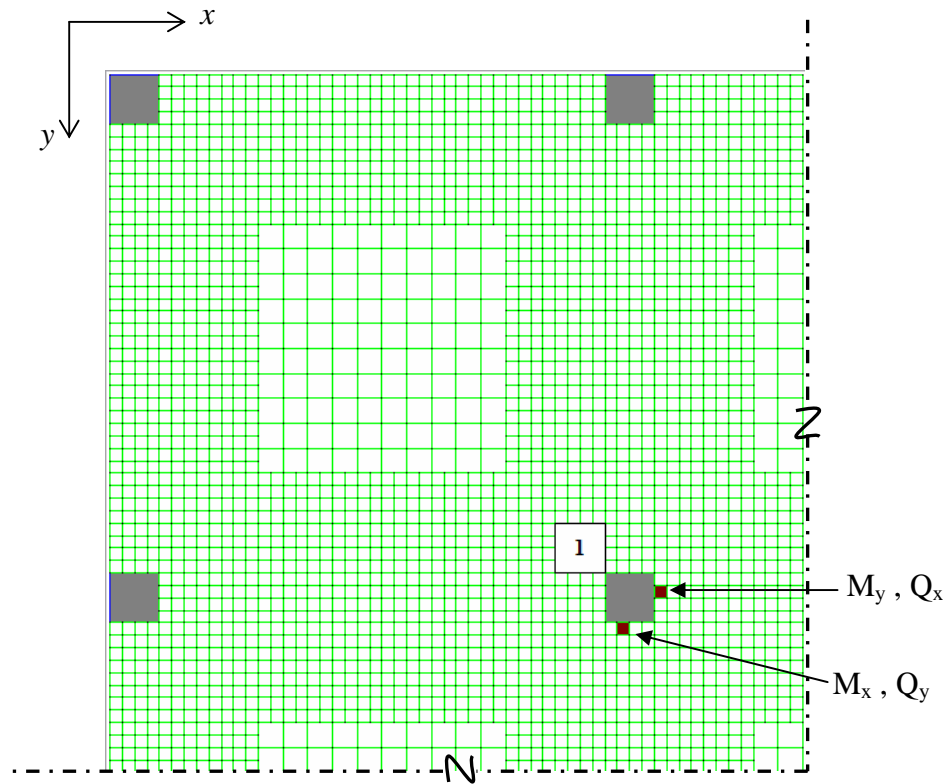


**Figure 18** Location of maximum stress resultant with opening number 1

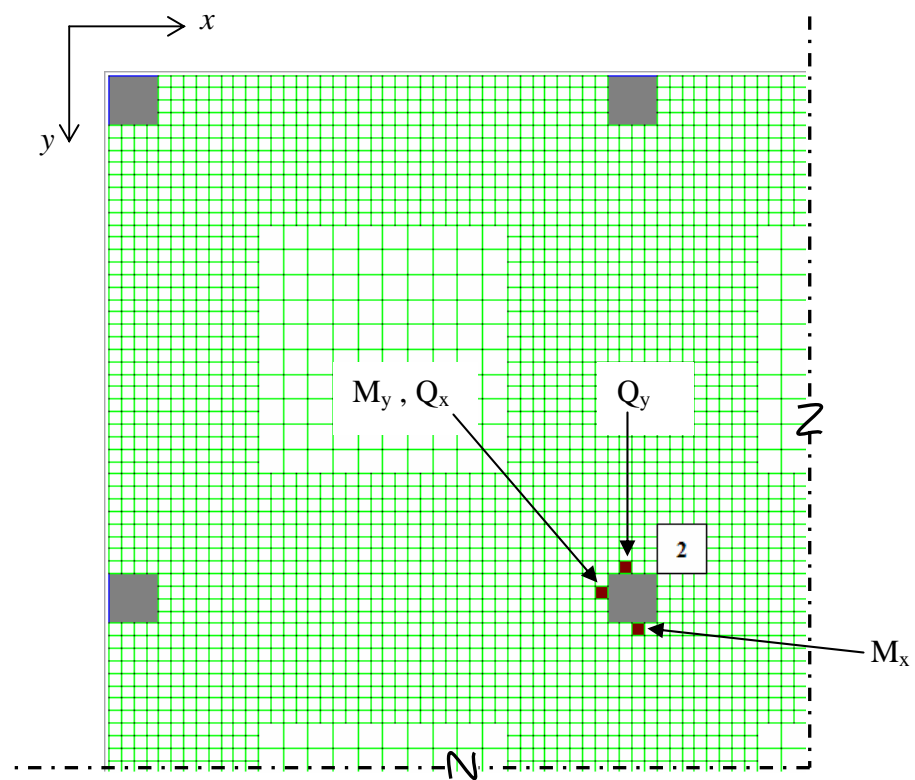


**Figure 19** Location of maximum stress resultant with opening number 2

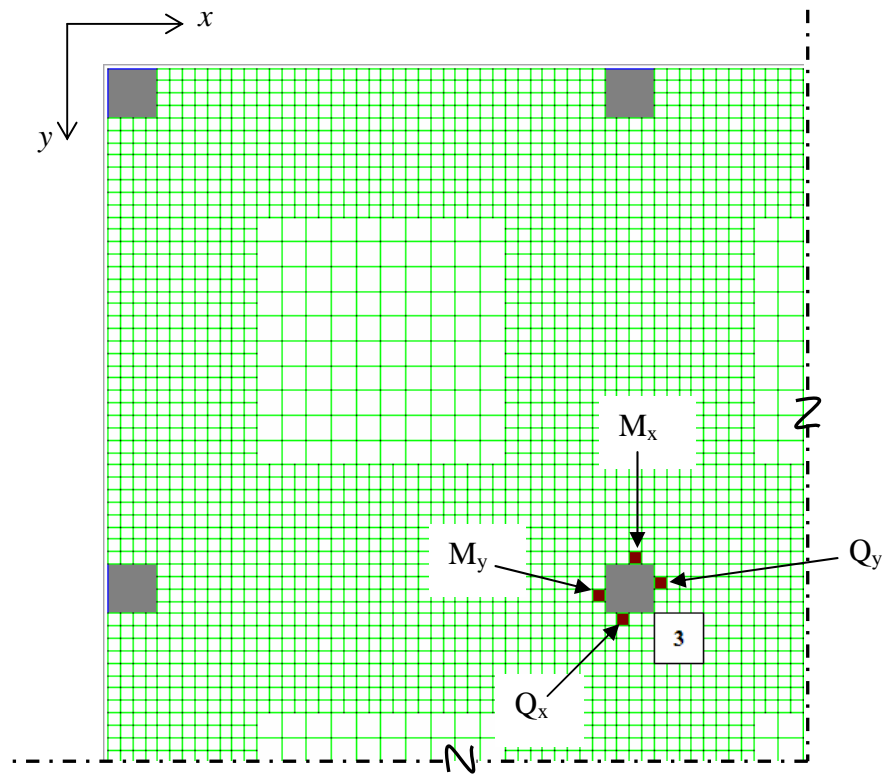


**Figure 20** Location of maximum stress resultant with opening number 3

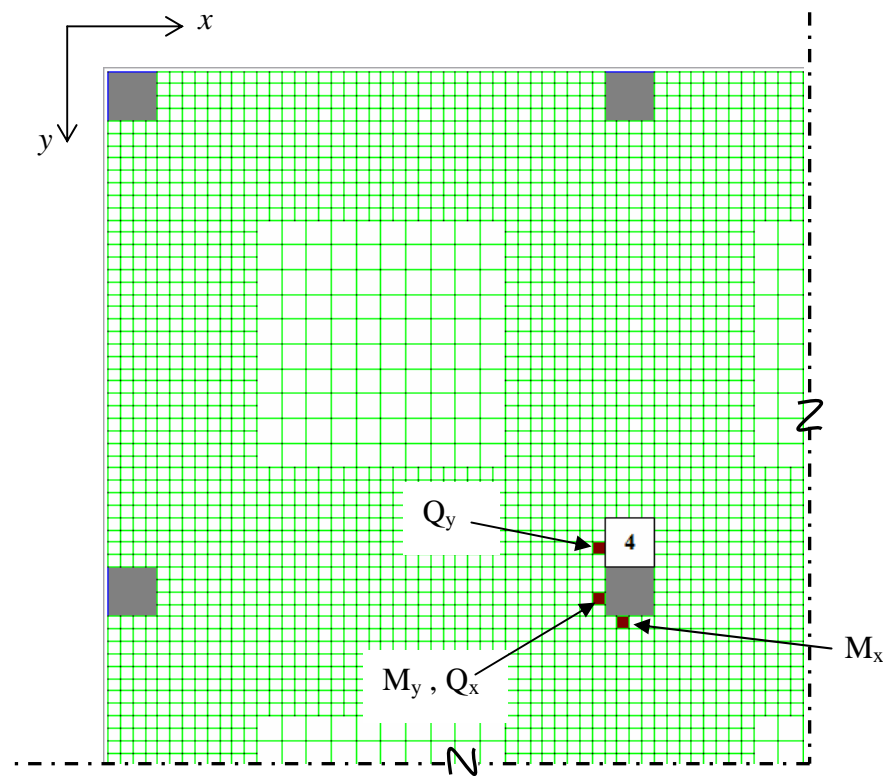


**Figure 21** Location of maximum stress resultant with opening number 4

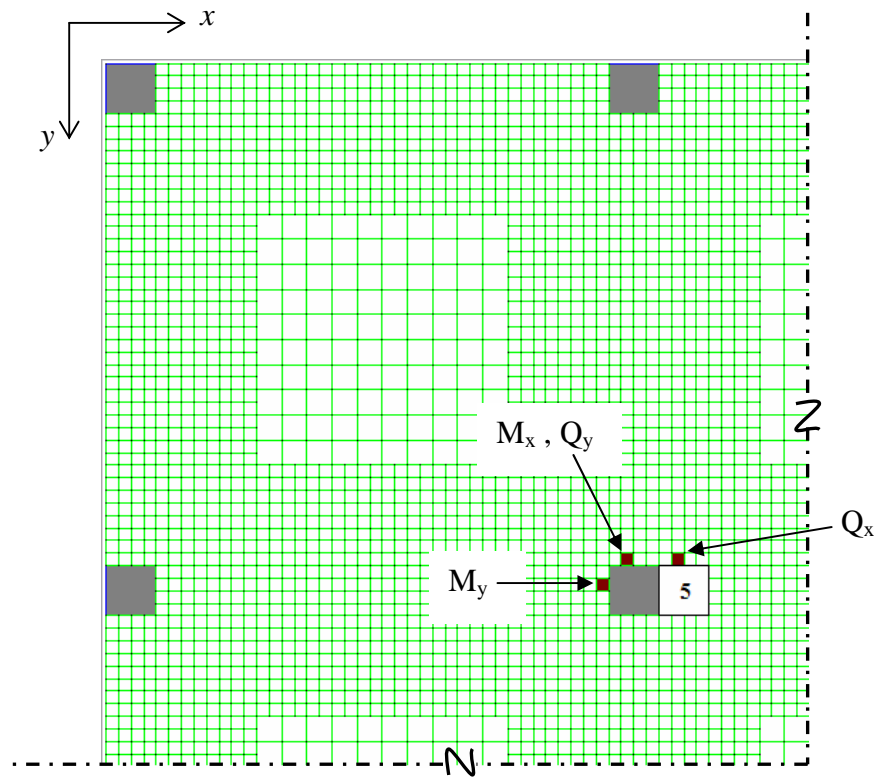


**Figure 22** Location of maximum stress resultant with opening number 5

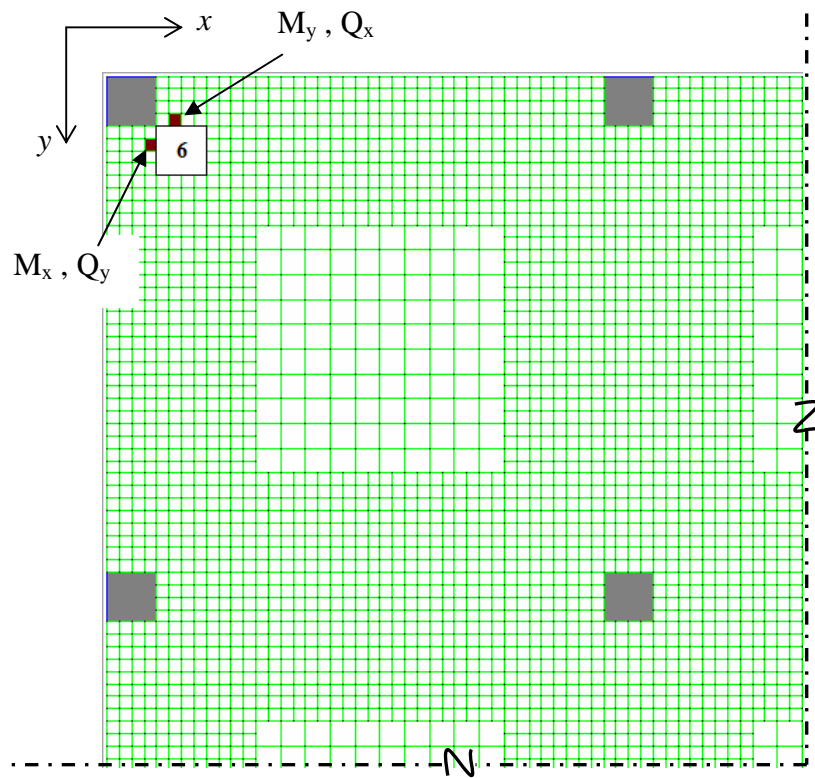


**Figure 23** Location of maximum stress resultant with opening number 6

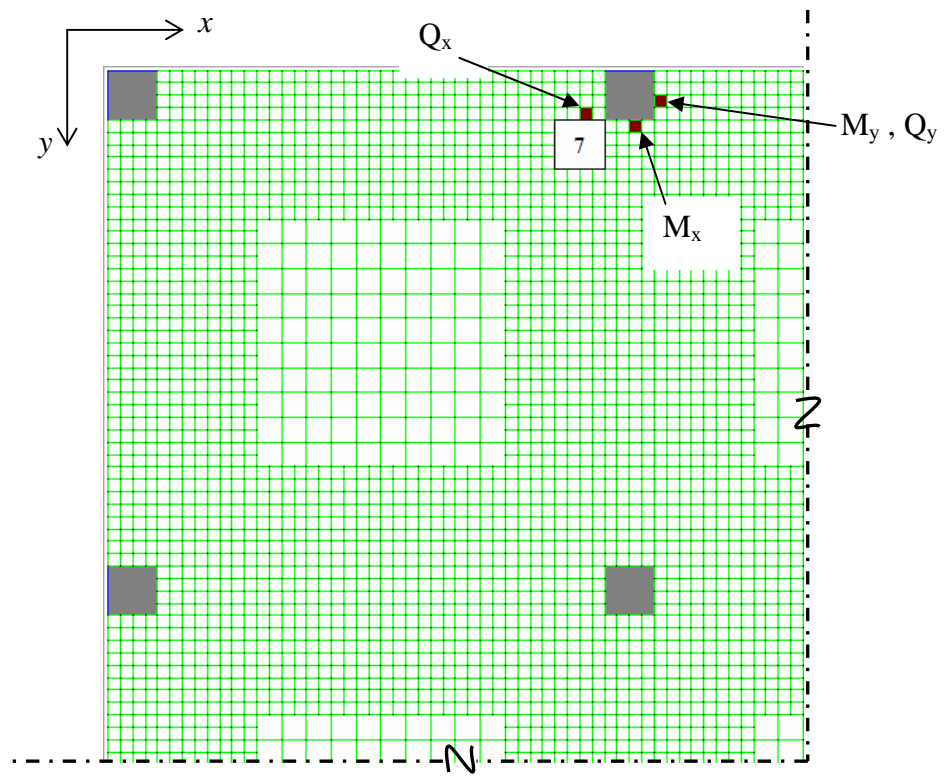


**Figure 24** Location of maximum stress resultant with opening number 7

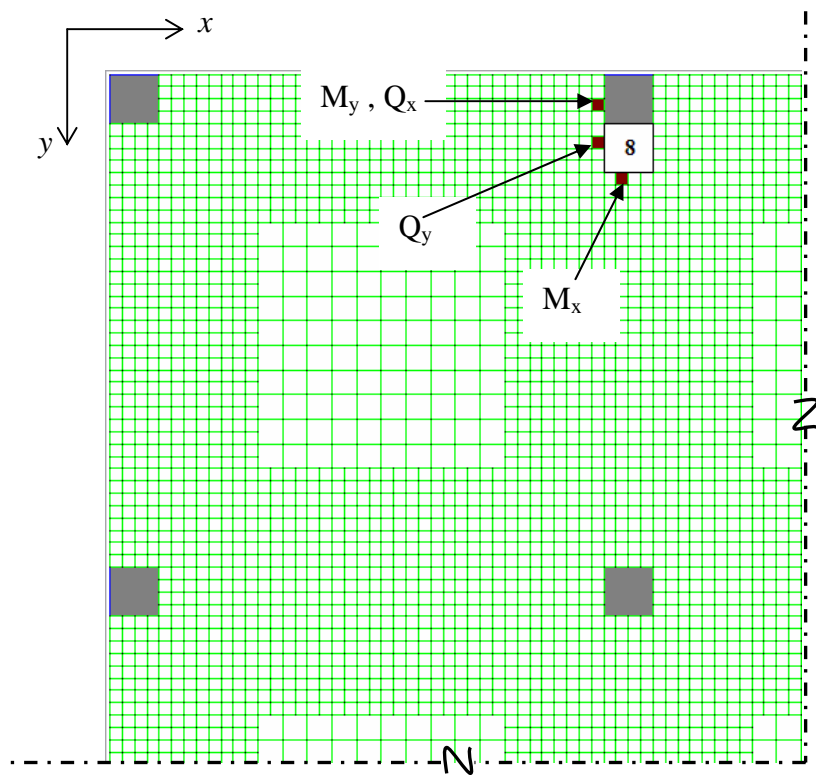


**Figure 25** Location of maximum stress resultant with opening number 8

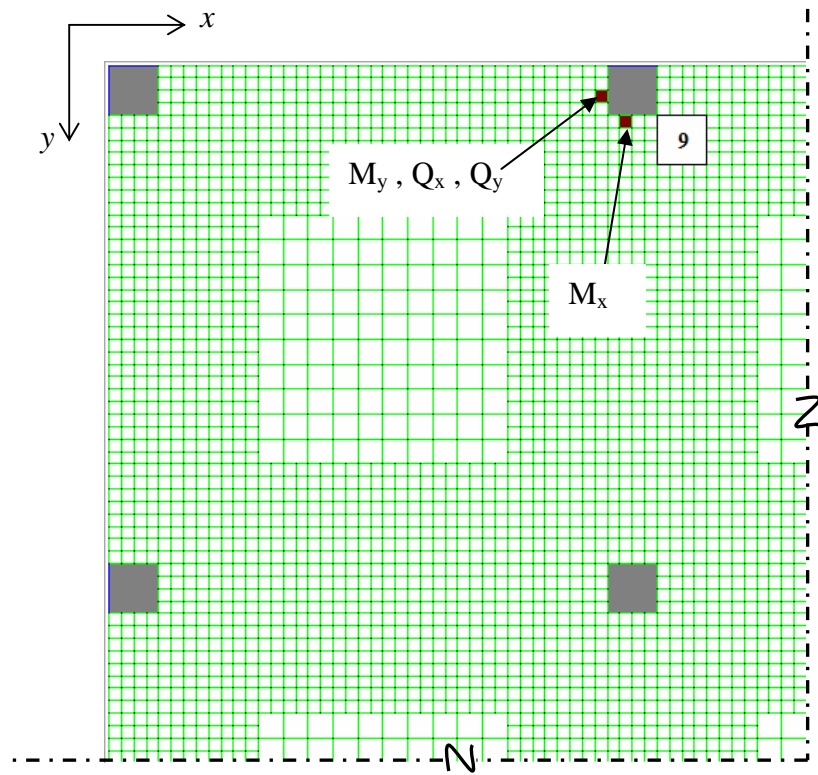


**Figure 26** Location of maximum stress resultant with opening number 9

### 3. Effect of Opening Size and Location on Stress Resultant Change

3.1 Analyze the flat plates with opening at the face of the column. The locations of the openings were classified into three categories. First, the opening at interior column and located at interior panel that is represented by “*in-in*” as shown in Figure 27. Second, the opening at interior column and located at exterior panel that is represented by “*in-ex*” as shown in Figure 28. Finally, the opening at edge column that is represented by “*edge*” as shown in Figure 29.

The data of flat plate for analysis used as the data as shown in Figure 16 are as follows:

Span	8	m
Thickness	0.25	m
Column width	0.80	m
Uniform load	1450	kg/m <sup>2</sup>
Concrete; E	21.72E6	kN/m <sup>2</sup>
ν	0.17	

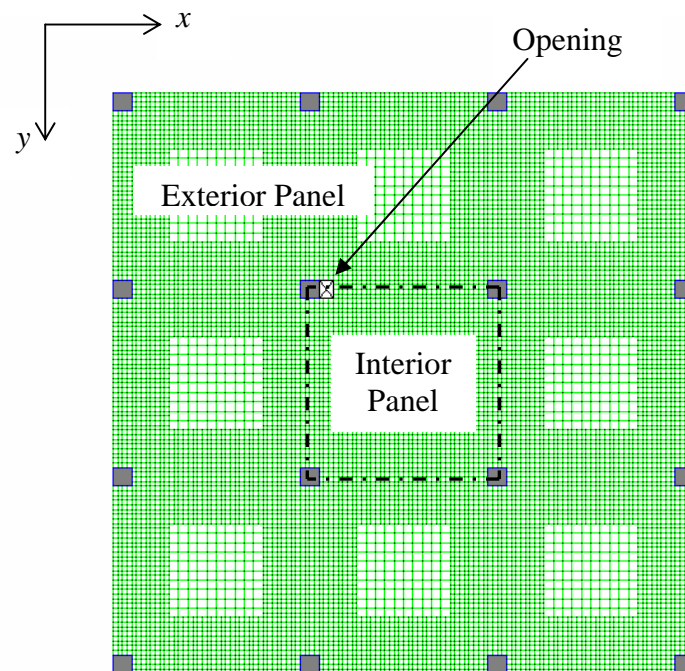


**Figure 27** Flat plate with opening at “*in-in*”

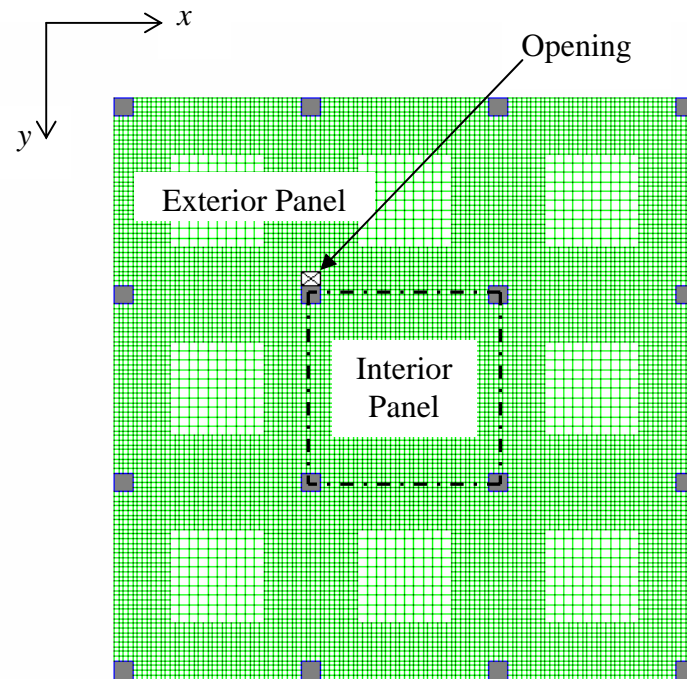


**Figure 28** Flat plate with opening at “*in-ex*”

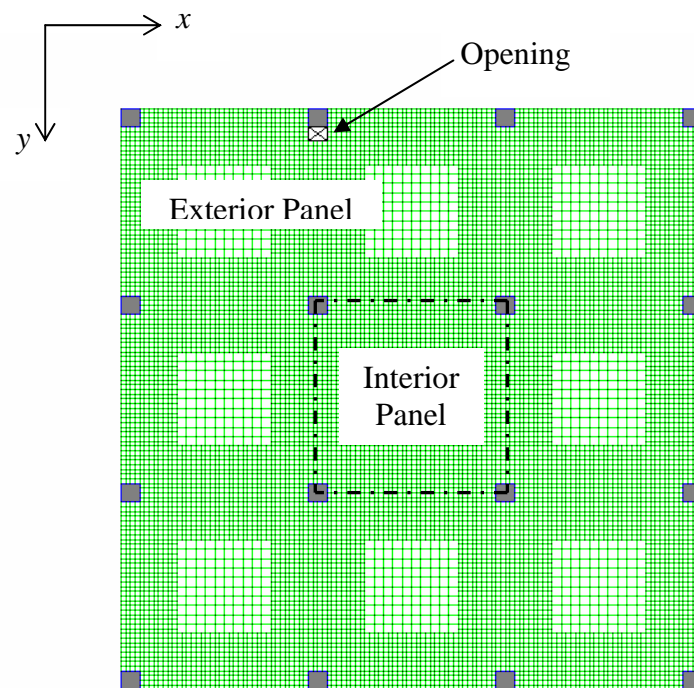


**Figure 29** Flat plate with opening at “*edge*”

First, analyze the flat plates with opening at interior column and located at interior panel. Then vary the size of openings at one-tenth, one-fifth, three-tenths, and two-fifths of the width of column strip into two direction of the plane of flat plate.

The dimension of the opening at interior column and located at interior panel is shown in Figure 30 represented by  $a$  and  $b$ . The dimension  $a$  is the width of opening in perpendicular direction of the face of column. The dimension  $b$  is the width of opening in parallel direction of the face of column.

The width of column strip is 4 m, and the size of openings are one-tenth, one-fifth, three-tenths, and two-fifths of the width of column strip then the size of opening is equal to 0.40 m, 0.80 m, 1.20 m, and 1.60 m respectively.

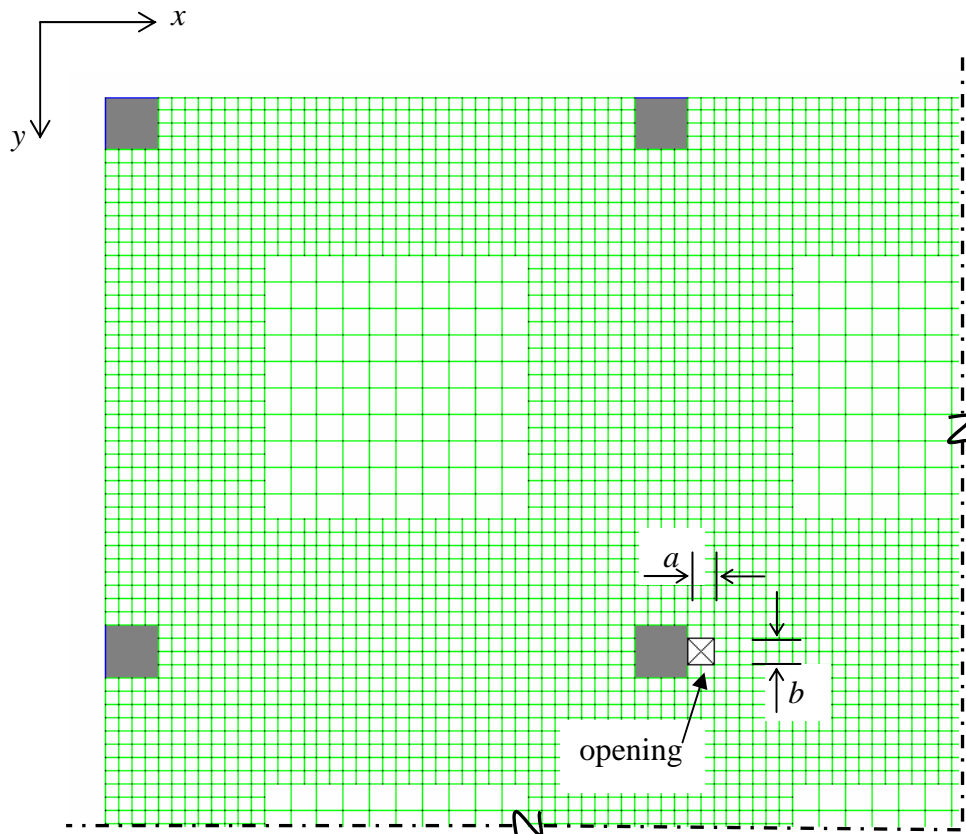


**Figure 30** Size of the opening at “*in-in*”

**Table 4** Percentage of maximum stress resultants change of flat plate with opening at interior column and located at interior side

Size of Opening ( $a \times b$ )  (m $\times$ m)	Percentage of Maximum Stress Resultants Change (%)			
	$M_x$	$M_y$	$Q_x$	$Q_y$
0.4 $\times$ 0.4	3.23	6.45	7.33	7.59
0.8 $\times$ 0.4	5.53	11.98	14.26	14.56
1.2 $\times$ 0.4	7.37	16.13	18.87	19.28
1.6 $\times$ 0.4	8.29	18.89	18.36	22.56
0.4 $\times$ 0.8	5.99	11.52	59.13	16.31
0.8 $\times$ 0.8	8.29	17.05	20.87	22.67
1.2 $\times$ 0.8	9.22	20.74	24.72	26.51
1.6 $\times$ 0.8	10.14	22.58	27.23	29.03
0.4 $\times$ 1.2	11.98	21.66	67.69	35.03
0.8 $\times$ 1.2	12.90	25.35	33.69	38.31
1.2 $\times$ 1.2	13.36	27.65	34.51	40.15
1.6 $\times$ 1.2	13.28	29.03	35.85	41.33
0.4 $\times$ 1.6	14.29	30.41	71.59	48.31
0.8 $\times$ 1.6	14.75	32.72	41.79	49.59
1.2 $\times$ 1.6	14.75	34.10	42.82	50.15
1.6 $\times$ 1.6	14.75	34.56	43.28	50.41

In Table 4, the percentage of stress resultants change of flat plate with opening at interior column and located at interior panel can be illustrated by relationship between percentage of maximum stress resultants change and size of opening as shown in Figures 31 to 34.

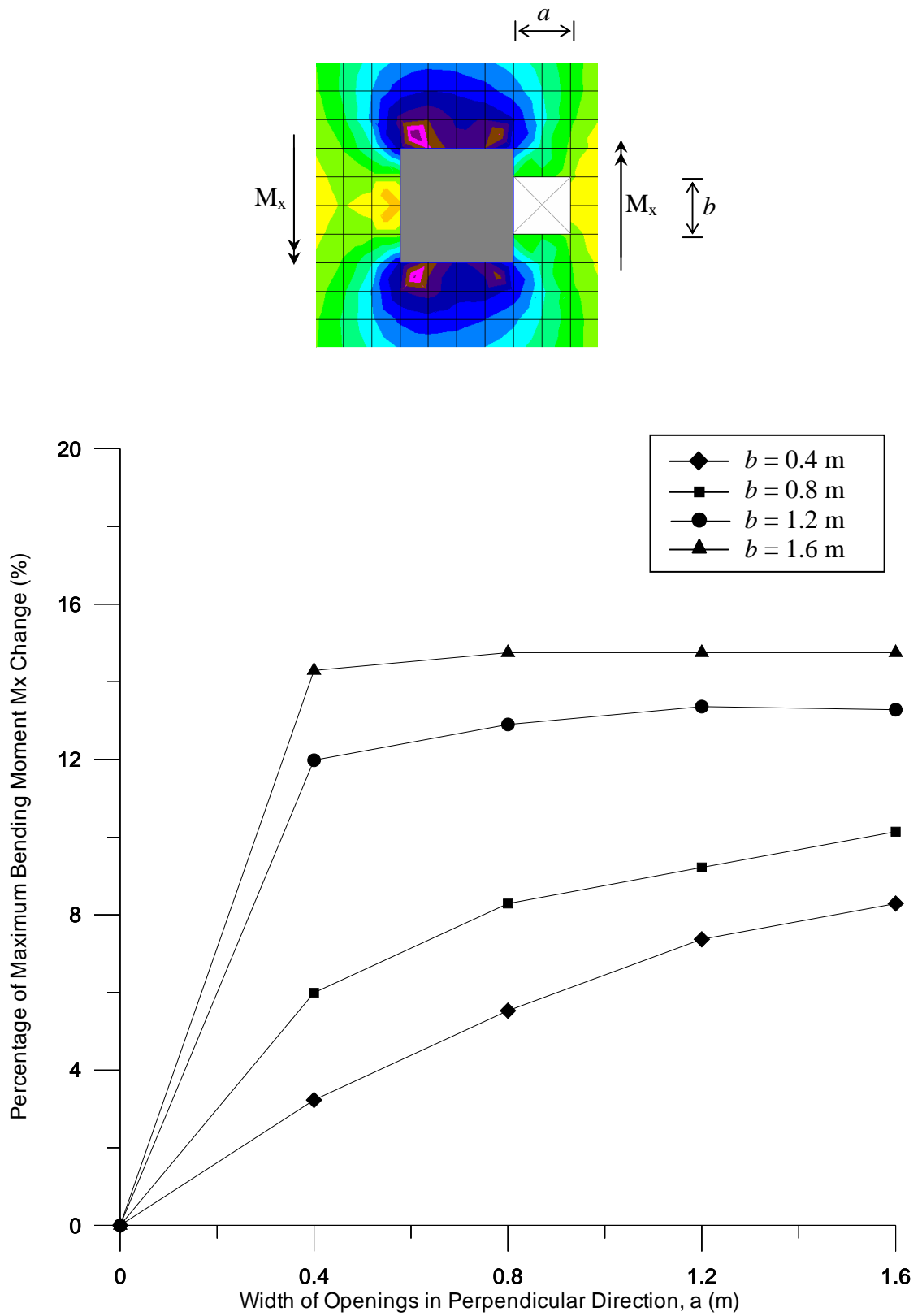


**Figure 31** Relationship between size of openings at “in-in” and percentage of maximum bending moment  $M_x$  change

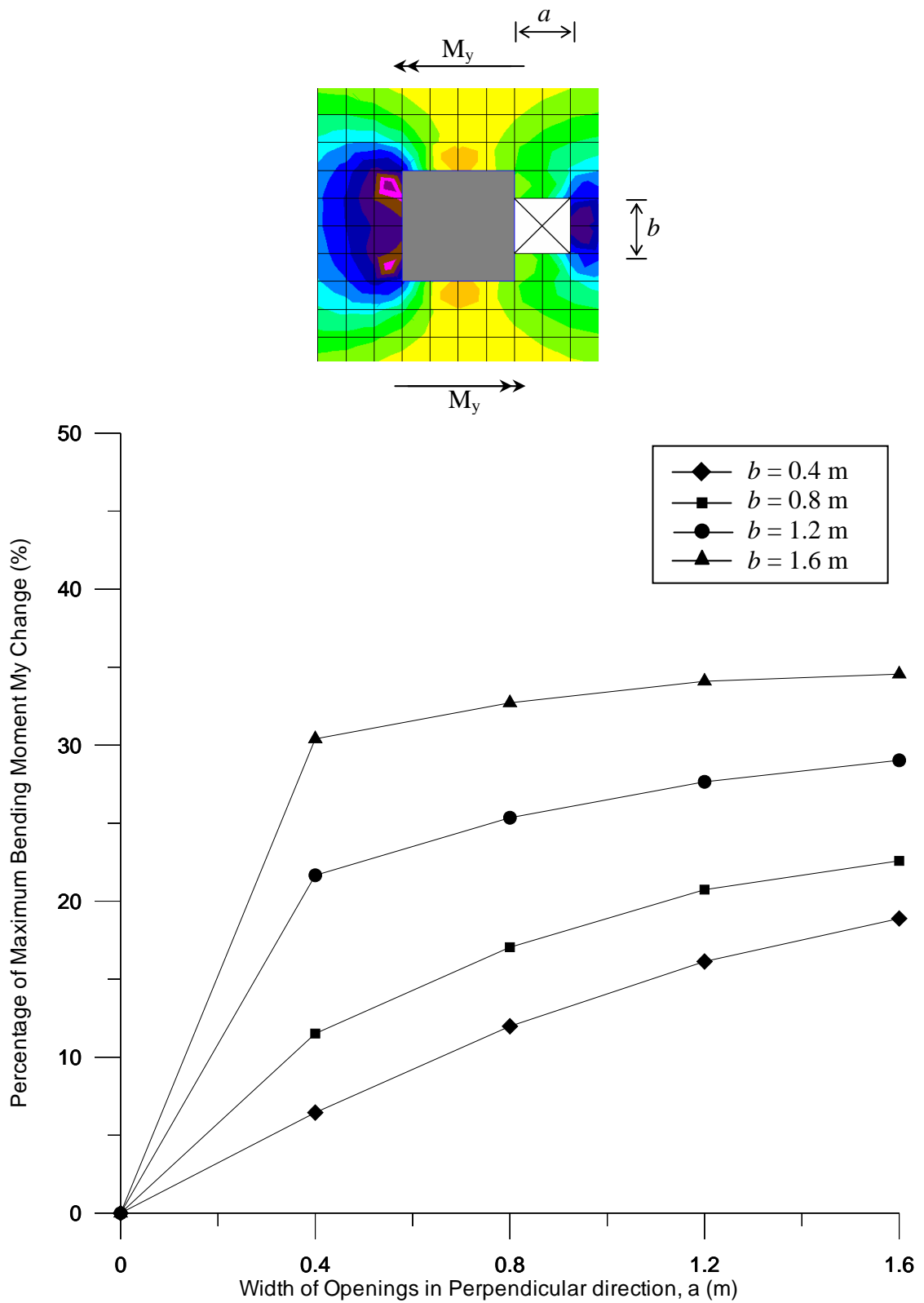


**Figure 32** Relationship between size of openings at “in-in” and percentage of maximum bending moment  $M_y$  change

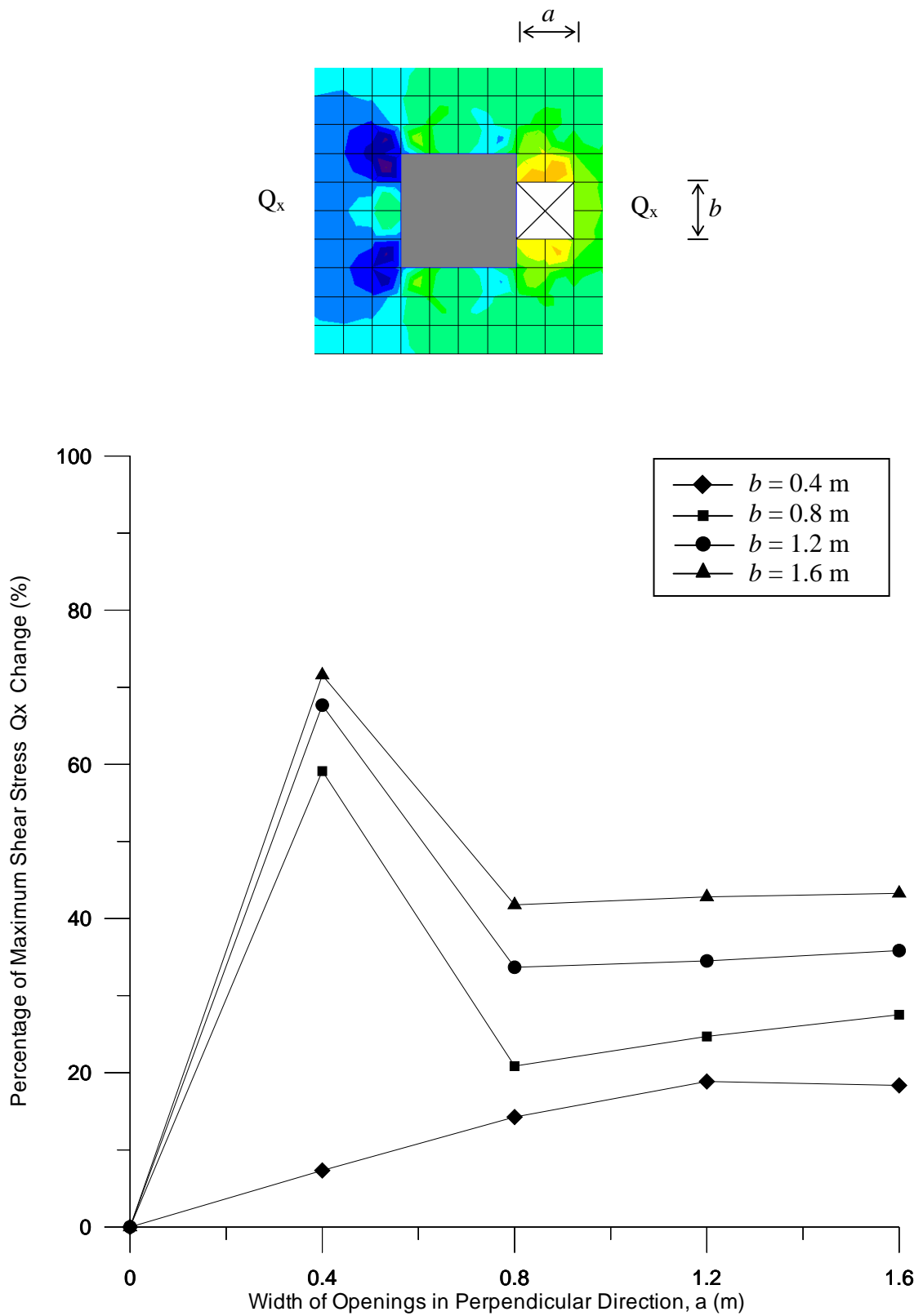


**Figure 33** Relationship between size of openings at “in-in” and percentage of maximum shear stress  $Q_x$  change

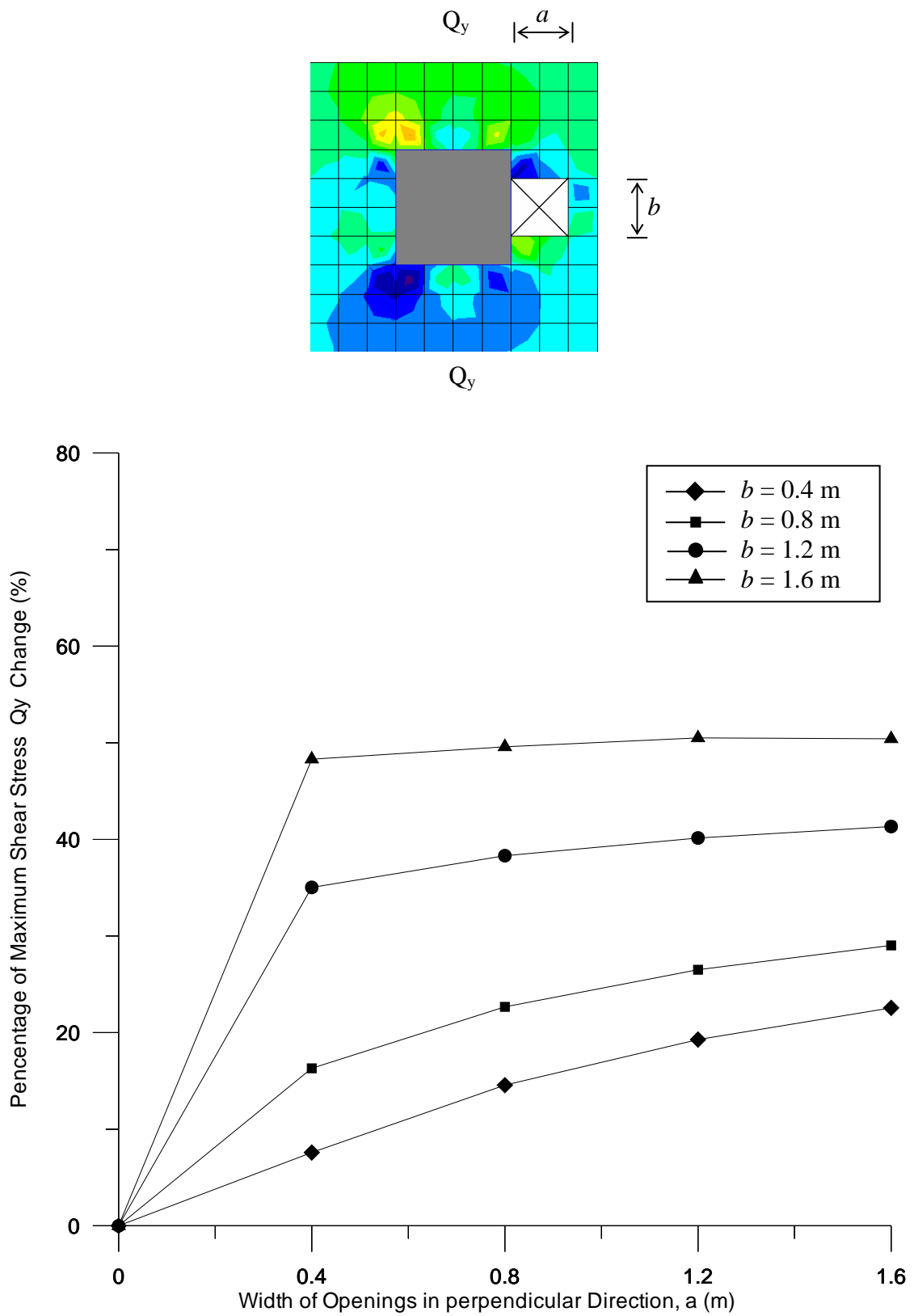


**Figure 34** Relationship between size of openings at “in-in” and percentage of maximum shear stress  $Q_y$  change

In Figure 31, at  $b = 0.4$  m the percentage of maximum bending moment change in  $x$  direction gradually increases from 3.23% to 8.29 % when the size of opening  $a$  is expanded from 0.4 m to 1.6 m. While  $a = 0.4$  m the percentage of maximum bending moment change in  $x$  direction will increase from 3.23% to 14.29 % when the size of opening  $b$  is expanded from 0.4 m to 1.6 m. When the width of opening  $b$  is equal to 1.6 m, the percentage of maximum bending moment  $M_x$  change is increases and flat out at 14.75%. Thus, the size of opening affected the maximum bending moment  $M_x$  when the opening is expanded in parallel direction of the face of the column and maximum bending moment  $M_x$  concentrated at the corner of column opposite side of the opening as shown in Figure 35. The percentage of maximum moment  $M_x$  change is rather constant when size of opening expanded in “ $a$ ” direction because it is parallel to the column strip in that direction.

The relationship between percentage of maximum bending moment  $M_y$  change and size of openings in Figure 32 are similar as bending moment  $M_x$  but percentage of  $M_y$  change is greater than  $M_x$ . Similarly the width  $b$  of opening is equal to 1.6 m the percentage of maximum bending moment  $M_y$  change gradually increases at 30.41% to 34.56%. The maximum bending moment  $M_y$  concentrated at the face of column opposite side of the opening as shown in Figure 36.

Percentage of maximum shear stress  $Q_x$  change is illustrated in Figure 33. It increased rapidly when the opening expanded in parallel direction of the face of column. At the size of opening  $a = 0.4$  m and  $b = 1.6$  m, the percentage of maximum shear stress  $Q_x$  change increase is equal to 71.59%. The maximum shear stress  $Q_x$  concentrated at the corner of opening and propagated to the corner of column opposite side of the opening as shown in Figure 37. But the openings expanded in perpendicular direction of the face of column, shear stress was reduced and flat out.

In Figure 34, the percentage of maximum shear stress  $Q_y$  change will increase to about 50% when openings expand in parallel direction of the face of column but are rather constant when expanding in perpendicular direction. Maximum shear stress  $Q_y$  concentrated at four corners of column as shown in Figure 38.

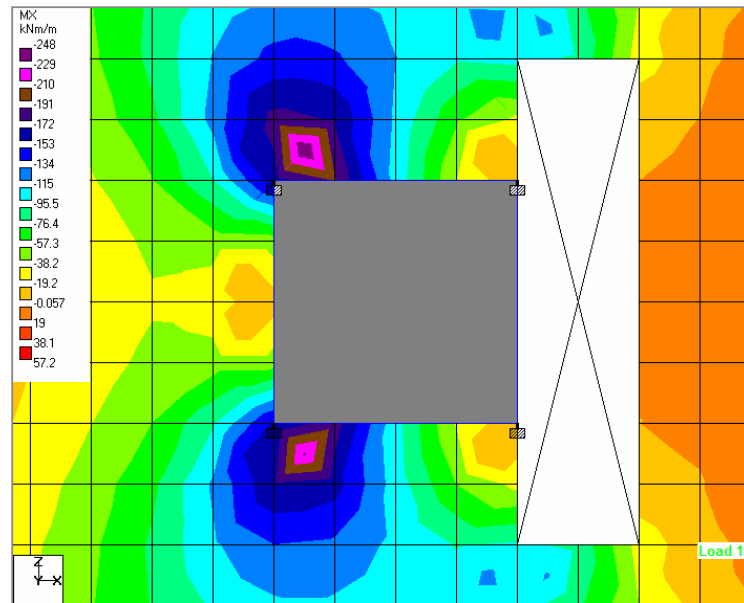


**Figure 35** Bending moment  $M_x$  concentration when opening  $a = 0.4$  m and  $b = 1.6$  m at “in-in”

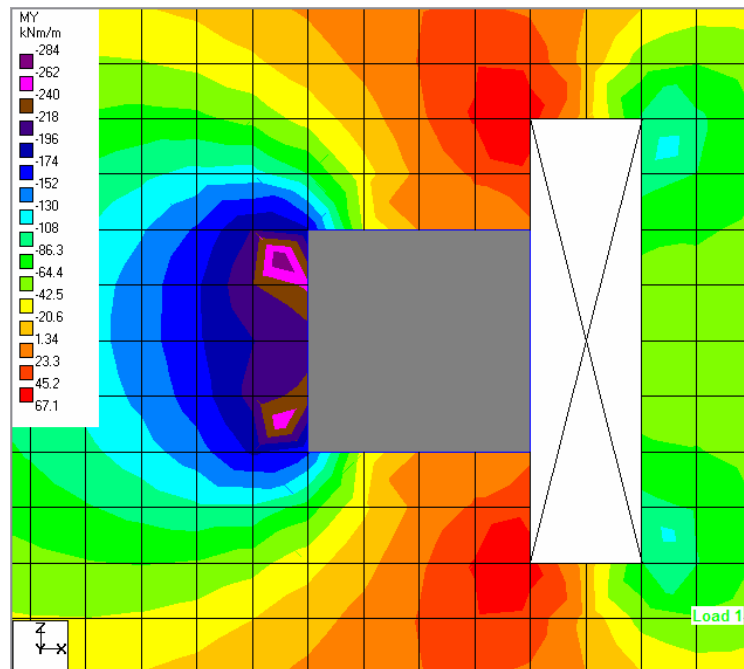


**Figure 36** Bending moment  $M_y$  concentration when opening  $a = 0.4$  m and  $b = 1.6$  m at “in-in”

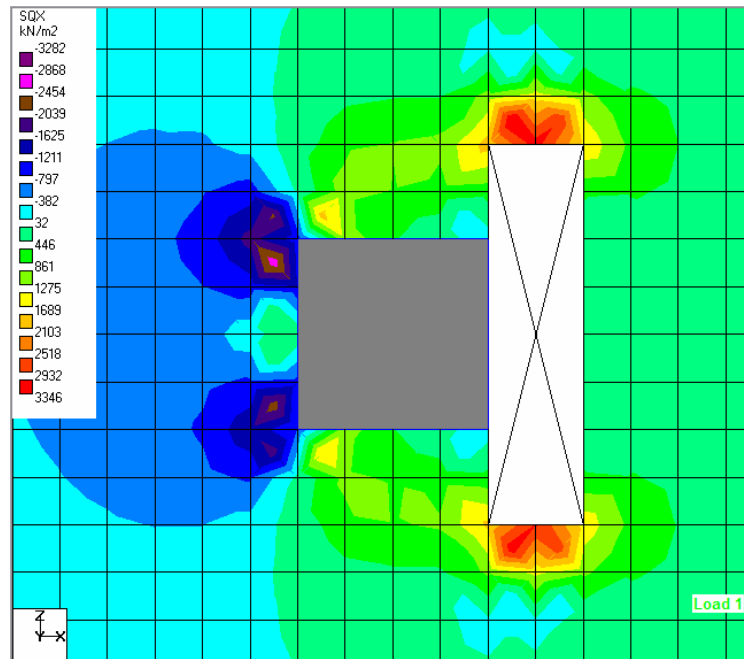


**Figure 37** Shear stress  $Q_x$  concentration when opening  $a = 0.4$  m and  $b = 1.6$  m at “in-in”

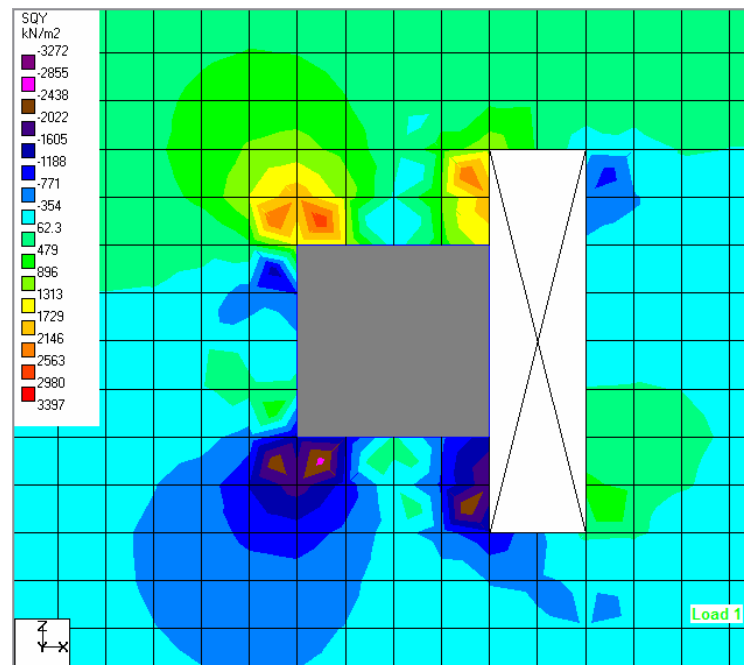


**Figure 38** Shear stress  $Q_y$  concentration when opening  $a = 0.4$  m and  $b = 1.6$  m at “in-in”

Next, analyze the flat plates for opening at interior column and located at exterior panel. Then vary the size of openings at one-tenth, one-fifth, three-tenths, and two-fifths of the width of column strip into two directions of the plane of flat plate.

The dimension of the opening at interior column and located at exterior panel is shown in Figure 39 represented by  $a$  and  $b$ . The dimension  $a$  is the width of opening in perpendicular direction of the face of column. The dimension  $b$  is the width of opening in parallel direction of the face of column.

The width of column strip is 4 m, and the size of openings are one-tenth, one-fifth, three-tenths, and two-fifths of the width of column strip then the size of openings are equal to 0.40 m, 0.80 m, 1.20 m, and 1.60 m respectively.

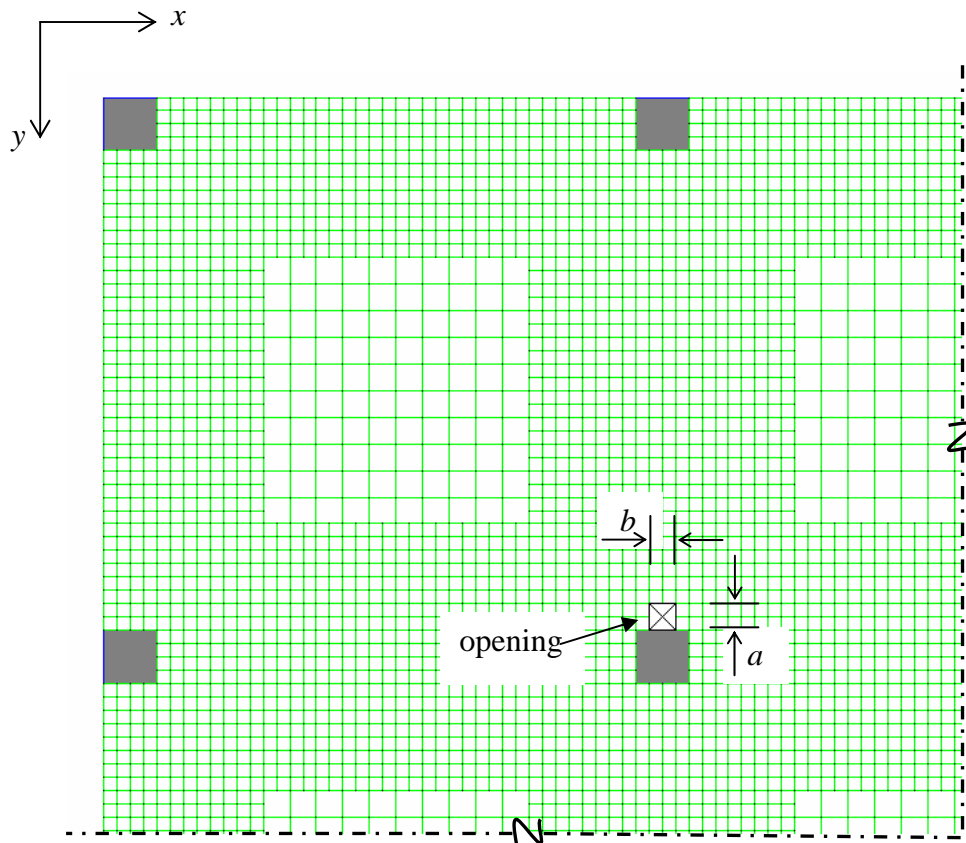


**Figure 39** Size of the opening at “in-ex”

**Table 5** Percentage of maximum stress resultants change of flat plate with opening at interior column and located at exterior side

Size of Opening ( $a \times b$ )  (m $\times$ m)	Percentage of Maximum Stress Resultant Change (%)			
	$M_x$	$M_y$	$Q_x$	$Q_y$
0.4 $\times$ 0.4	1.38	-3.69	-7.90	10.31
0.8 $\times$ 0.4	7.37	-3.23	-0.62	8.36
1.2 $\times$ 0.4	11.52	-1.84	0.41	11.33
1.6 $\times$ 0.4	14.29	-0.46	0.46	14.62
0.4 $\times$ 0.8	7.37	-2.76	1.49	74.21
0.8 $\times$ 0.8	12.90	-0.46	8.10	34.82
1.2 $\times$ 0.8	16.59	0.46	12.05	17.59
1.6 $\times$ 0.8	18.89	1.38	14.72	20.21
0.4 $\times$ 1.2	17.97	3.69	59.23	81.82
0.8 $\times$ 1.2	22.12	5.07	36.56	46.15
1.2 $\times$ 1.2	24.42	5.53	27.49	29.64
1.6 $\times$ 1.2	25.81	5.99	28.72	29.85
0.4 $\times$ 1.6	27.65	5.99	46.31	83.44
0.8 $\times$ 1.6	29.95	6.45	38.05	50.97
1.2 $\times$ 1.6	31.34	6.91	38.62	37.54
1.6 $\times$ 1.6	31.80	6.91	38.87	38.00

In Table 5, the percentage of maximum stress resultants change of flat plate with opening at interior column and located at exterior panel can be illustrated by relationship between percentage of maximum stress resultants change and size of opening as shown in Figures 40 to 43.

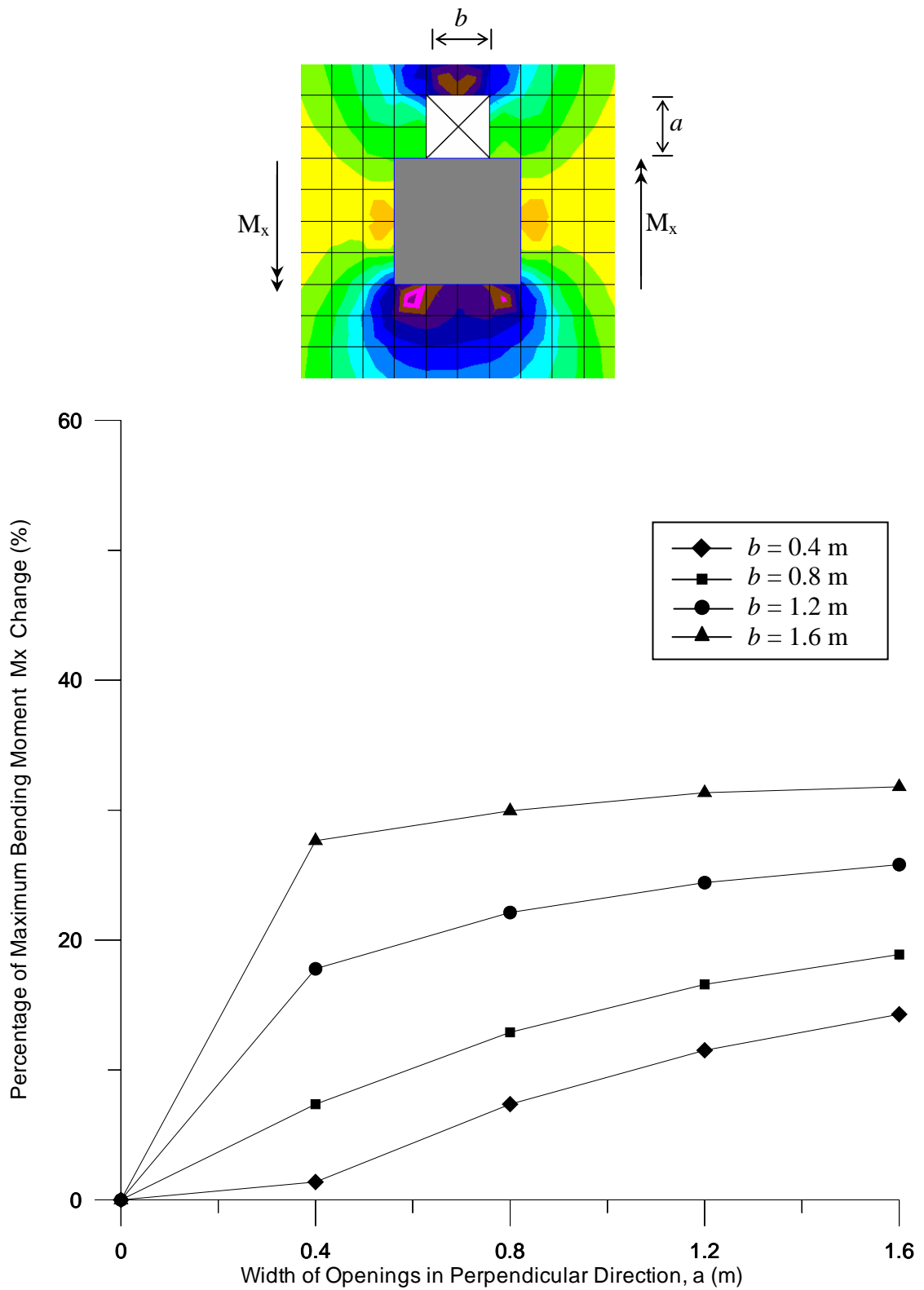


**Figure 40** Relationship between size of openings at “*in-ex*” and percentage of maximum bending moment  $M_x$  change

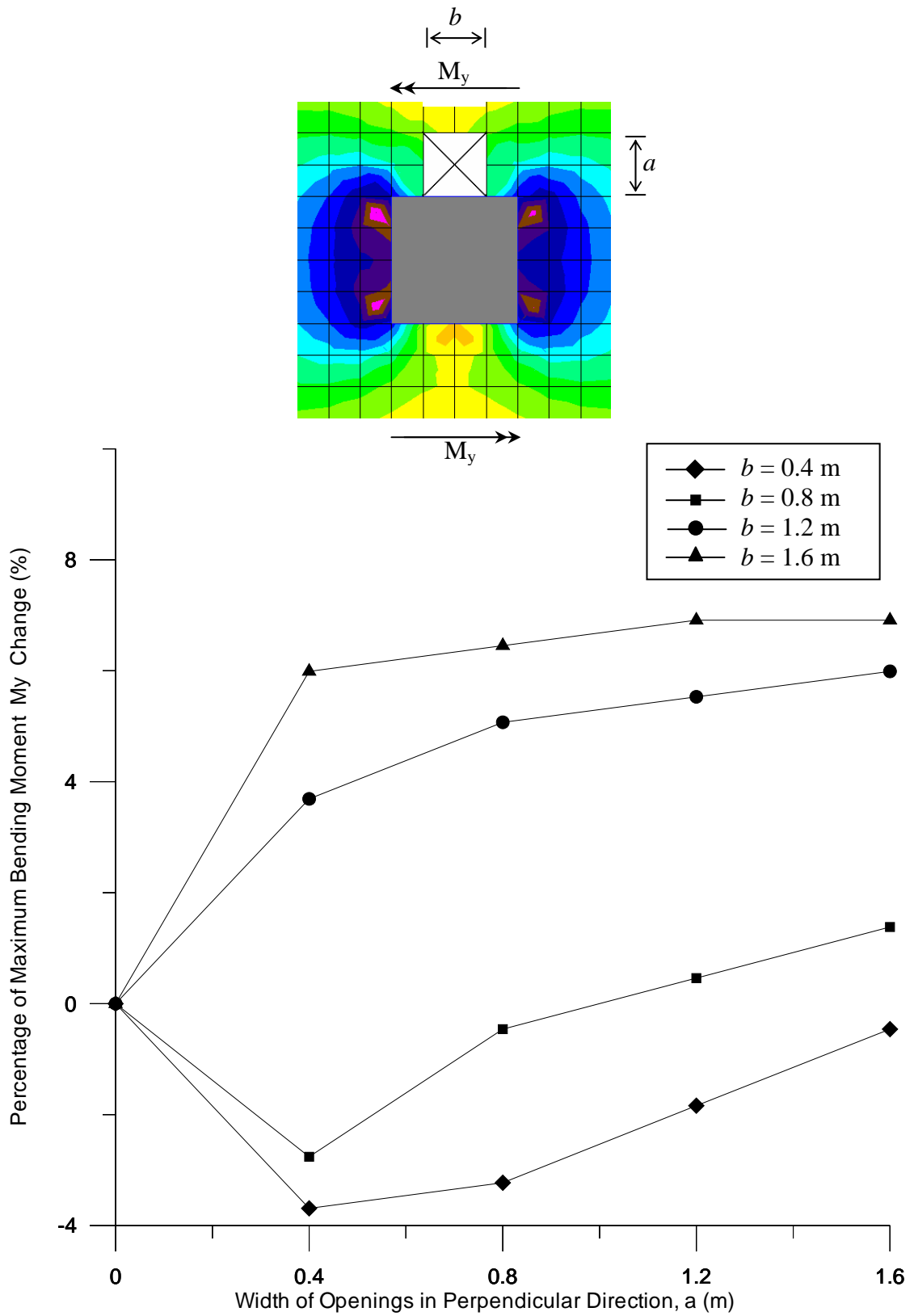


**Figure 41** Relationship between size of openings at “*in-ex*” and percentage of maximum bending moment  $M_y$  change

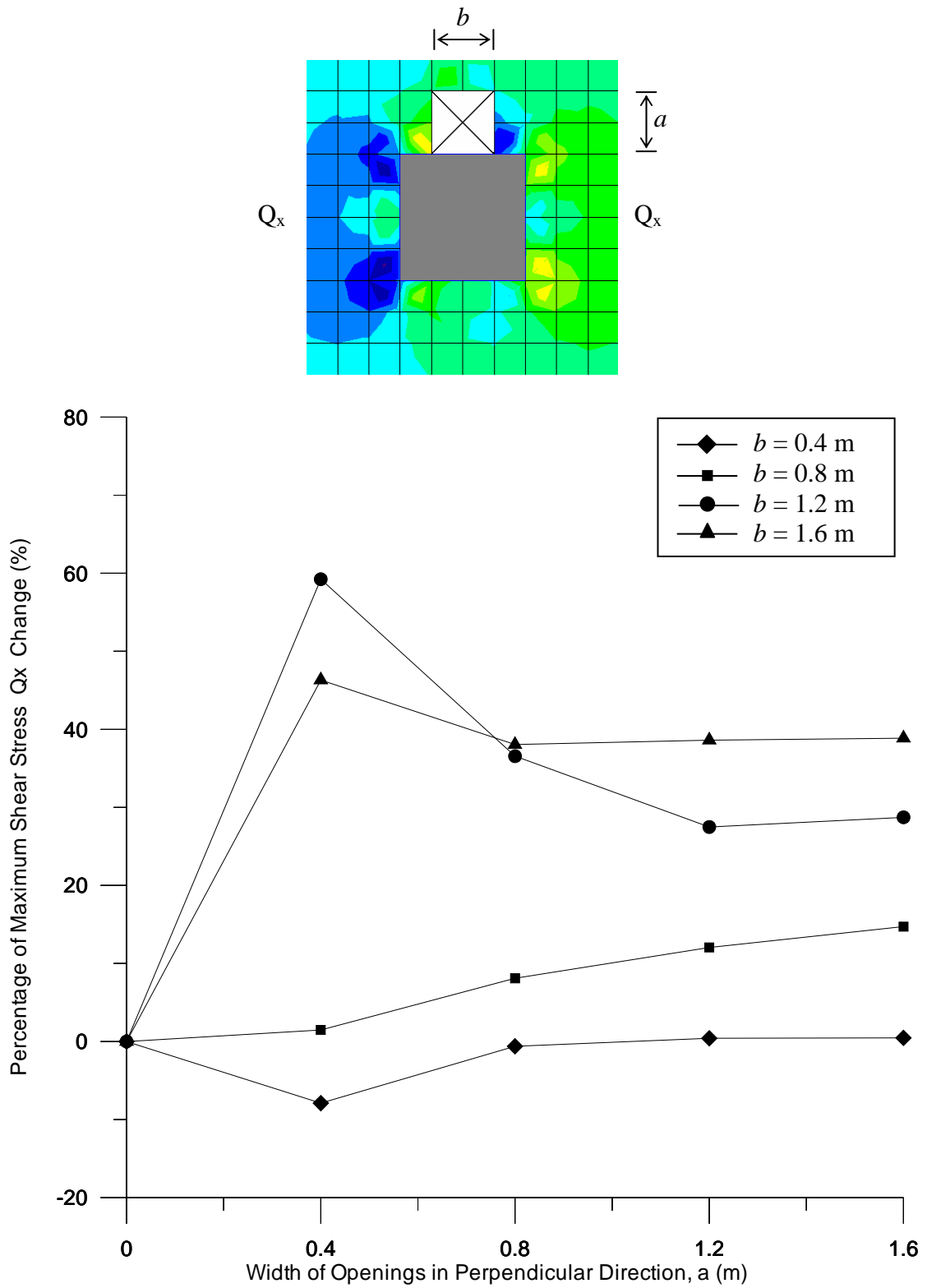


**Figure 42** Relationship between size of openings at “*in-ex*” and percentage of maximum shear stress  $Q_x$  change

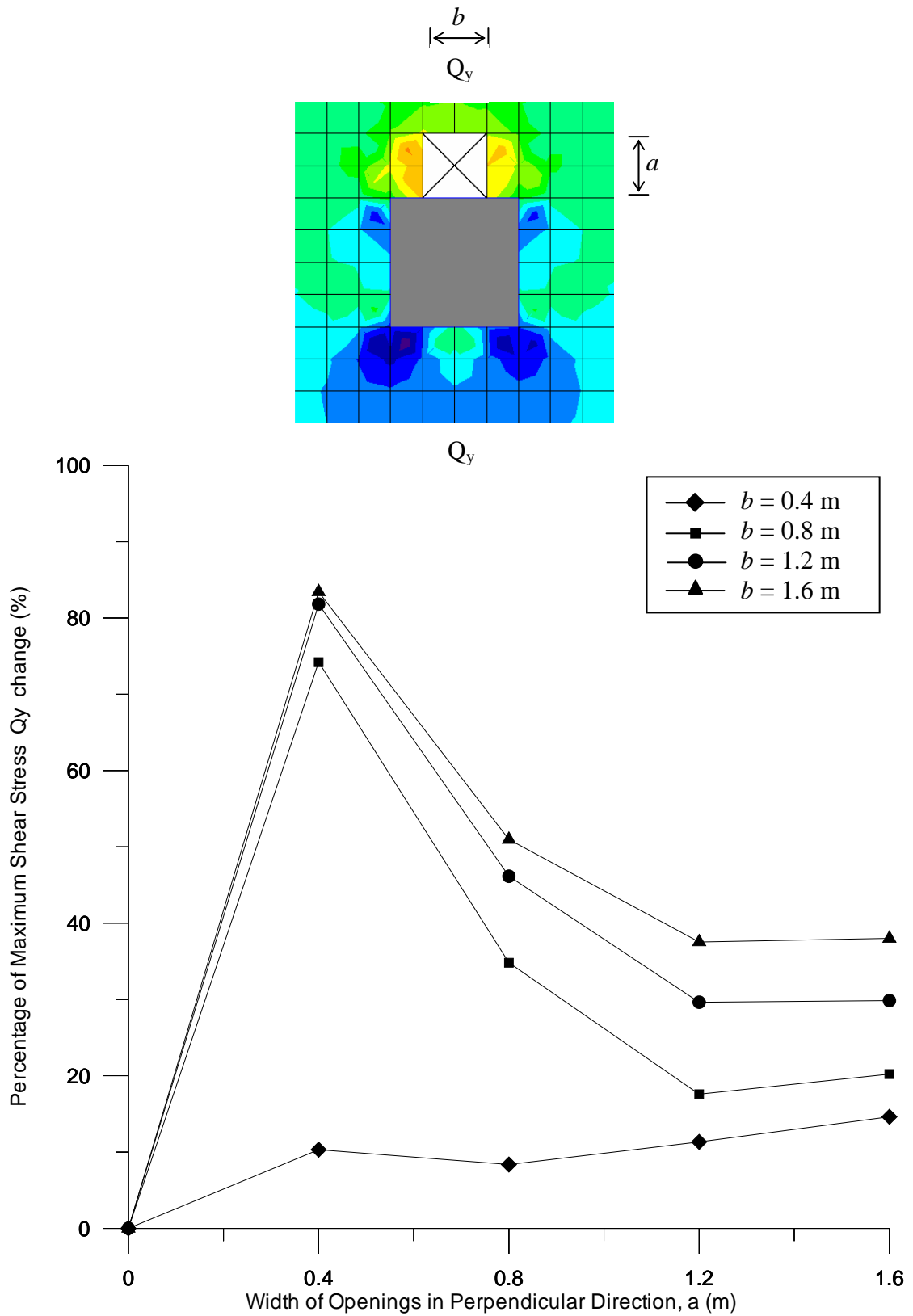


**Figure 43** Relationship between size of openings at “in-ex” and percentage of maximum shear stress  $Q_y$  change

In Figure 40, at  $b = 0.4$  m the percentage of maximum bending moment change in  $x$  direction gradually increases from 1.38% to 14.29 % when the size of opening  $a$  expands from 0.4 m to 1.6 m. While  $a = 0.4$  m the percentage of maximum bending moment change in  $x$  direction will increase from 1.38% to 27.65 % when the size of opening  $b$  expands from 0.4 m to 1.6 m respectively. The width  $b$  of opening is equal to 1.6 m the percentage of maximum bending moment  $M_x$  change gradually increases from 27.65% and saturated at 31.80% when size of opening  $a$  expands from 0.4 m to 1.6 m. Thus, the size of opening affected to the bending moment  $M_x$  when the opening expands in parallel direction of the face of the column and maximum bending moment  $M_x$  concentrated at the face of column opposite side of the opening as shown in Figure 44.

At  $a = 0.4$  m, the percentage of maximum bending moment  $M_y$  change as shown in Figure 41 will reduced slightly -3.69% and -2.76% when the width of openings  $b = 0.4$  m and  $b = 0.8$  m respectively. It gradually increases to 1.38% and -0.46% when the size of opening  $a$  expands to 1.6 m. But maximum percentage of bending moment  $M_y$  change increased slightly 3.69% and 5.99% when the width of openings  $b = 1.2$  m and  $b = 1.6$  m respectively. It gradually increases to 5.99% and 6.91% when the size of opening  $a$  expands to 1.6 m. The maximum bending moment  $M_y$  concentrated at the corner of column opposite side of the opening is shown in Figure 45.

In Figure 42, percentage of maximum shear stress  $Q_x$  change will increase to 59.23% when opening  $a = 0.4$  m and  $b = 1.2$  m. When sizes of openings expand larger, the percentage of maximum shear stress  $Q_x$  change will reduced. Maximum shear stress  $Q_x$  concentrated at four corners of column as shown in Figure 46.

Maximum shear stress  $Q_y$  illustrated in Figure 43, increases rapidly when the opening expands in parallel direction of the face of column. At size of opening  $a = 0.4$  m and  $b = 1.6$  m, percentage of maximum shear stress  $Q_y$  change increase equal to 83.44%. When sizes of openings expand larger, the percentage of maximum shear stress  $Q_y$  change will be reduced. Maximum shear stress  $Q_y$  concentrated at the corner of opening and propagated to the corner of column opposite side of the opening as shown in Figure 47.

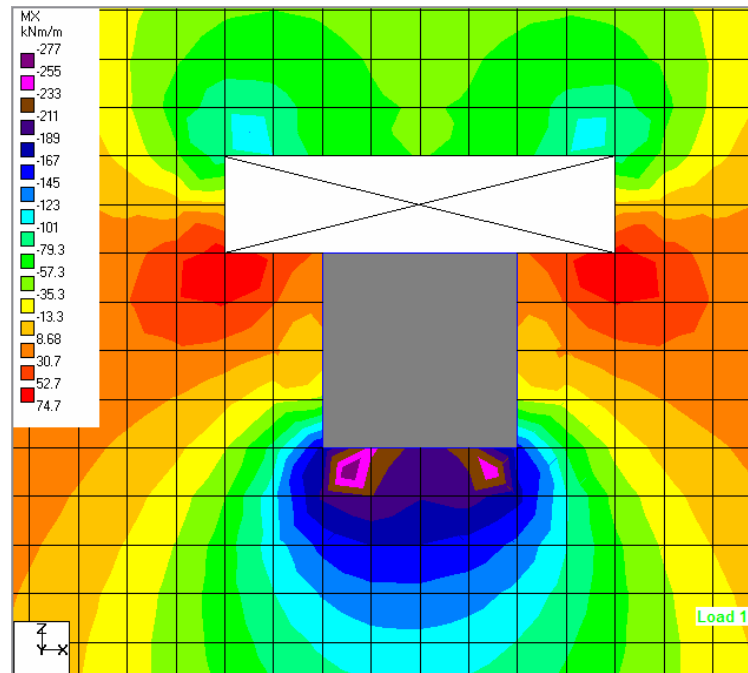


**Figure 44** Bending moment  $M_x$  concentration when opening  $a = 0.4$  m and  $b = 1.6$  m at “in-ex”

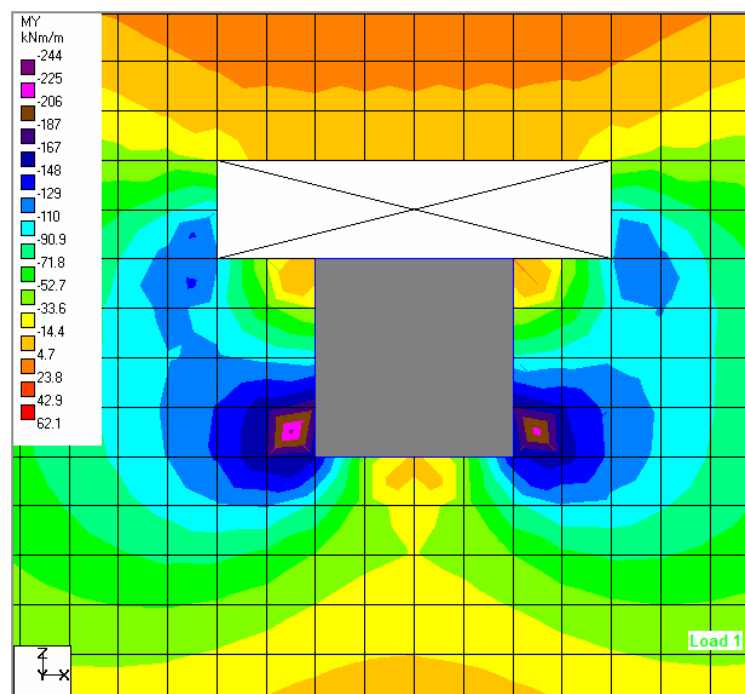


**Figure 45** Bending moment  $M_y$  concentration when opening  $a = 0.4$  m and  $b = 1.6$  m at “in-ex”

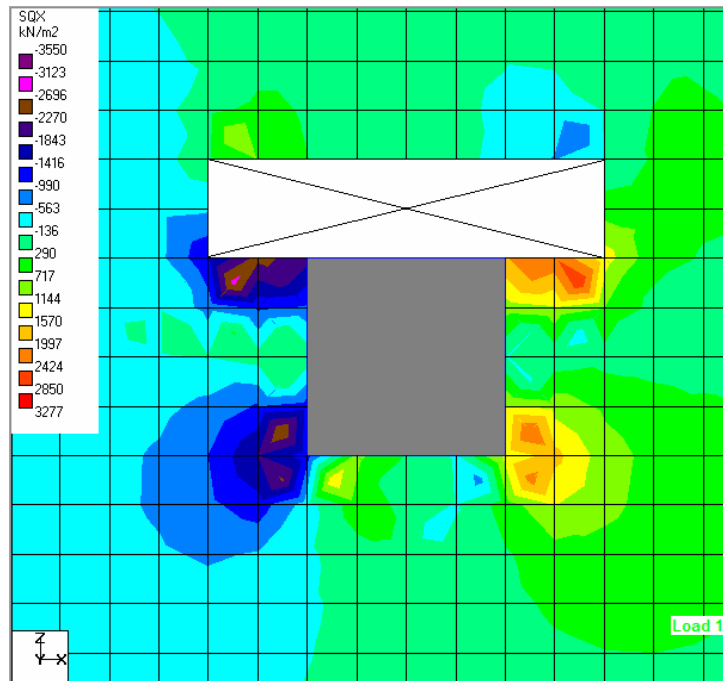


**Figure 46** Shear stress  $Q_x$  concentration when opening  $a = 0.4$  m and  $b = 1.6$  m at “in-ex”

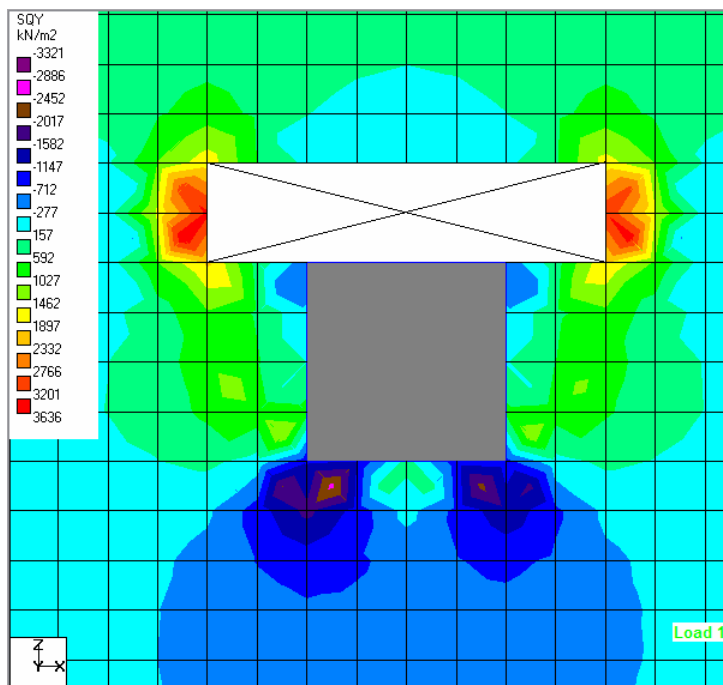


**Figure 47** Shear stress  $Q_y$  concentration when opening  $a = 0.4$  m and  $b = 1.6$  m at “in-ex”

Finally, analyze the flat plates for opening at edge column. Then vary the size of openings at one-tenth, one-fifth, three-tenths, and two-fifths of the width of column strip into two directions of the plane of flat plate.

The dimension of the opening at edge column is shown in Figure 48 represented by  $a$  and  $b$ . The dimension  $a$  is the width of opening in perpendicular direction of the face of column. The dimension  $b$  is the width of opening in parallel direction of the face of column.

The width of column strip is 4 m, and the size of openings are one-tenth, one-fifth, three-tenths, and two-fifths of the width of column strip then the size of openings are equal to 0.40 m, 0.80 m, 1.20 m, and 1.60 m respectively.

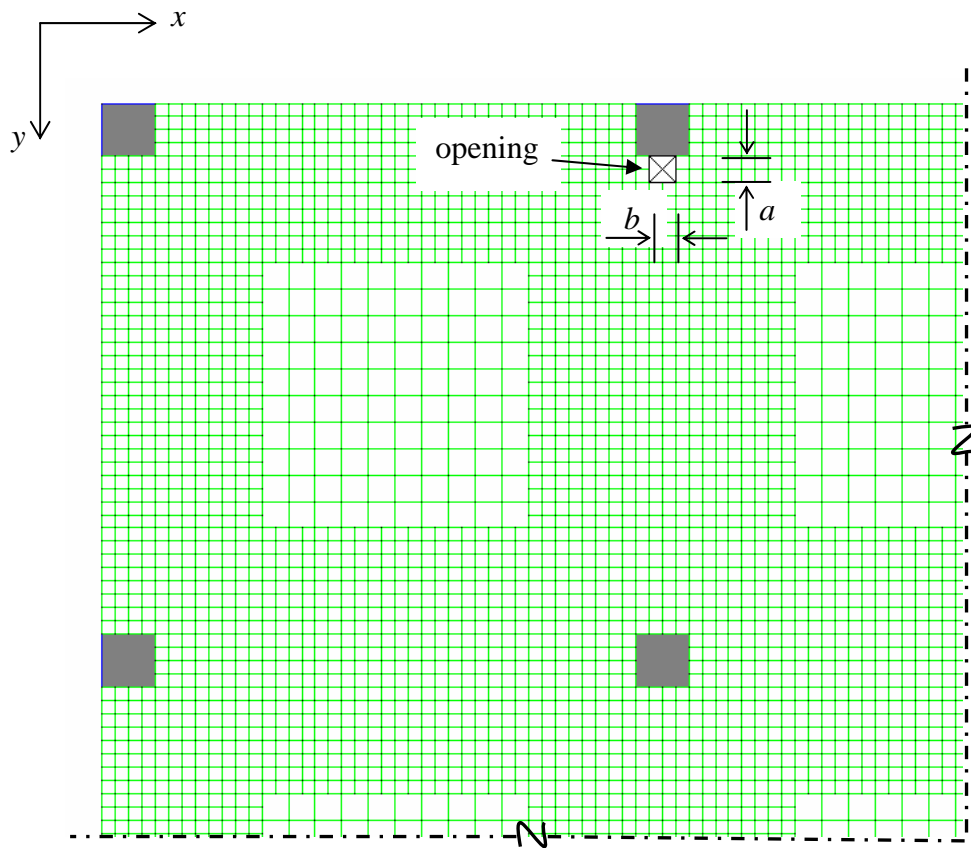


**Figure 48** Size of the opening at “edge”

**Table 6** Percentage of maximum stress resultants change of flat plate with opening at edge column

Size of Opening ( $a \times b$ )  (m $\times$ m)	Percentage of Maximum Stress Resultant Change (%)			
	$M_x$	$M_y$	$Q_x$	$Q_y$
0.4 $\times$ 0.4	-13.15	-1.80	-26.69	2.47
0.8 $\times$ 0.4	-22.07	-6.31	-27.93	4.12
1.2 $\times$ 0.4	-31.46	-9.91	-30.06	3.18
1.6 $\times$ 0.4	-40.38	-13.51	-31.91	1.41
0.4 $\times$ 0.8	-21.13	-18.92	-7.29	29.08
0.8 $\times$ 0.8	-33.80	-23.42	-8.71	8.80
1.2 $\times$ 0.8	-44.60	-26.58	-11.23	-0.24
1.6 $\times$ 0.8	-53.52	-29.28	-13.68	-5.71
0.4 $\times$ 1.2	-30.52	-29.28	62.12	34.51
0.8 $\times$ 1.2	-44.13	-30.18	53.91	15.27
1.2 $\times$ 1.2	-54.46	-32.43	48.05	6.57
1.6 $\times$ 1.2	-62.91	-34.68	43.46	1.16
0.4 $\times$ 1.6	-36.62	-45.05	101.14	35.22
0.8 $\times$ 1.6	-50.70	-44.59	88.63	16.37
1.2 $\times$ 1.6	-61.03	-45.95	80.35	7.91
1.6 $\times$ 1.6	-69.01	-46.85	74.13	2.54

In Table 6, the percentage of maximum stress resultants change of flat plate with opening at edge column can be illustrated by relationship between percentage of maximum stress resultants change and size of opening as shown in Figures 49 to 52.

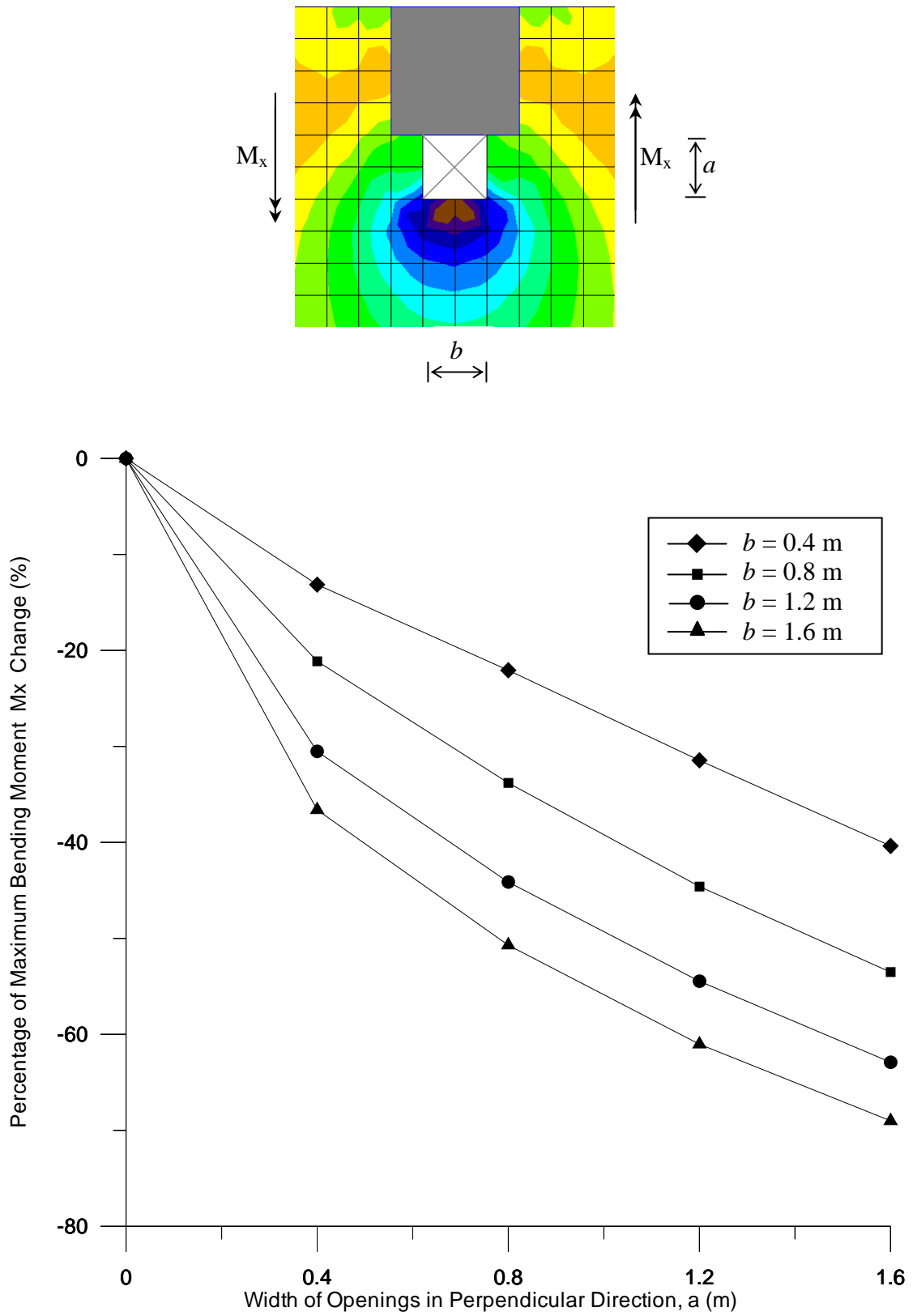


**Figure 49** Relationship between size of openings at “edge” and percentage of maximum bending moment  $M_x$  change

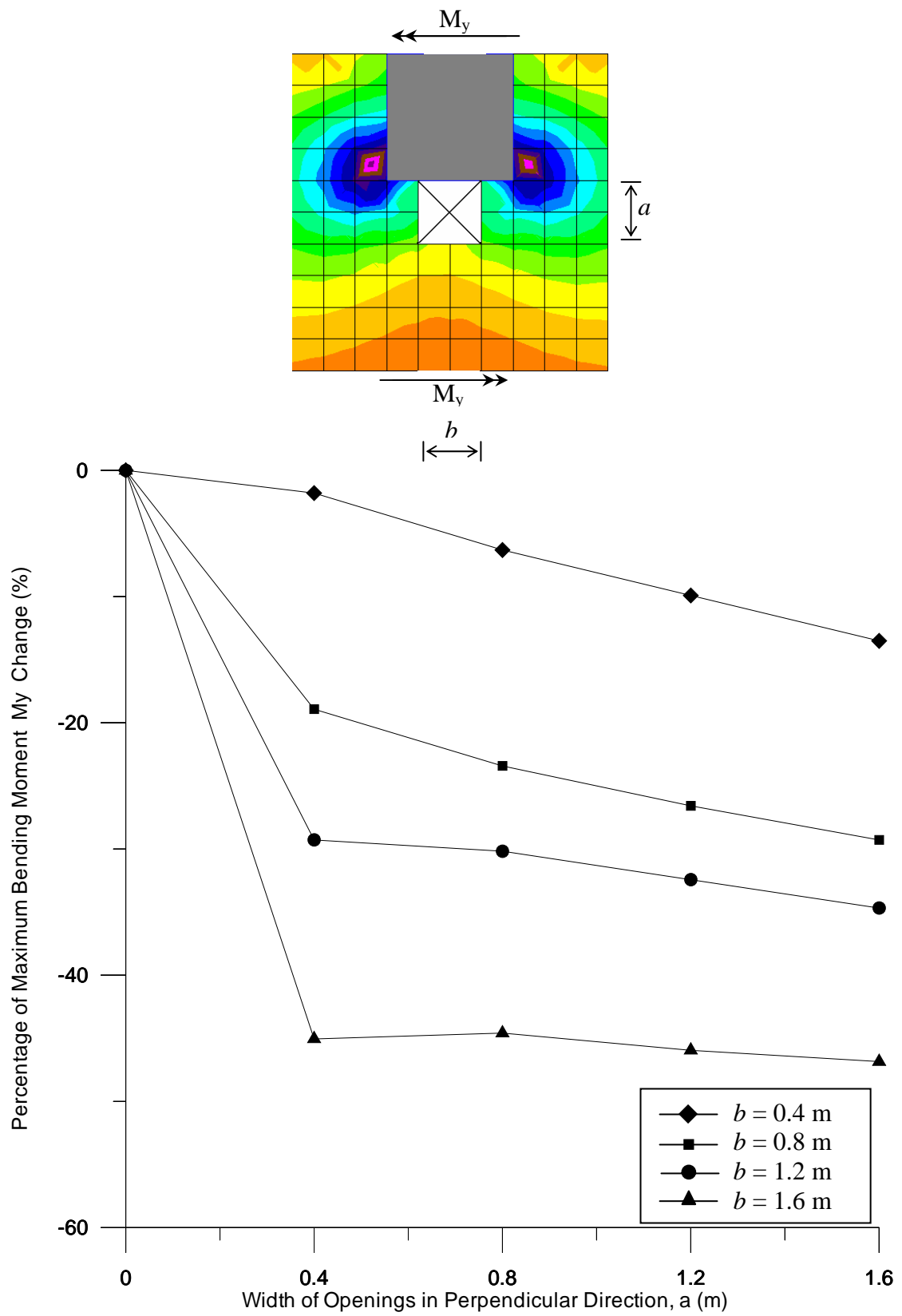


**Figure 50** Relationship between size of openings at “edge” and percentage of maximum bending moment  $M_y$  change

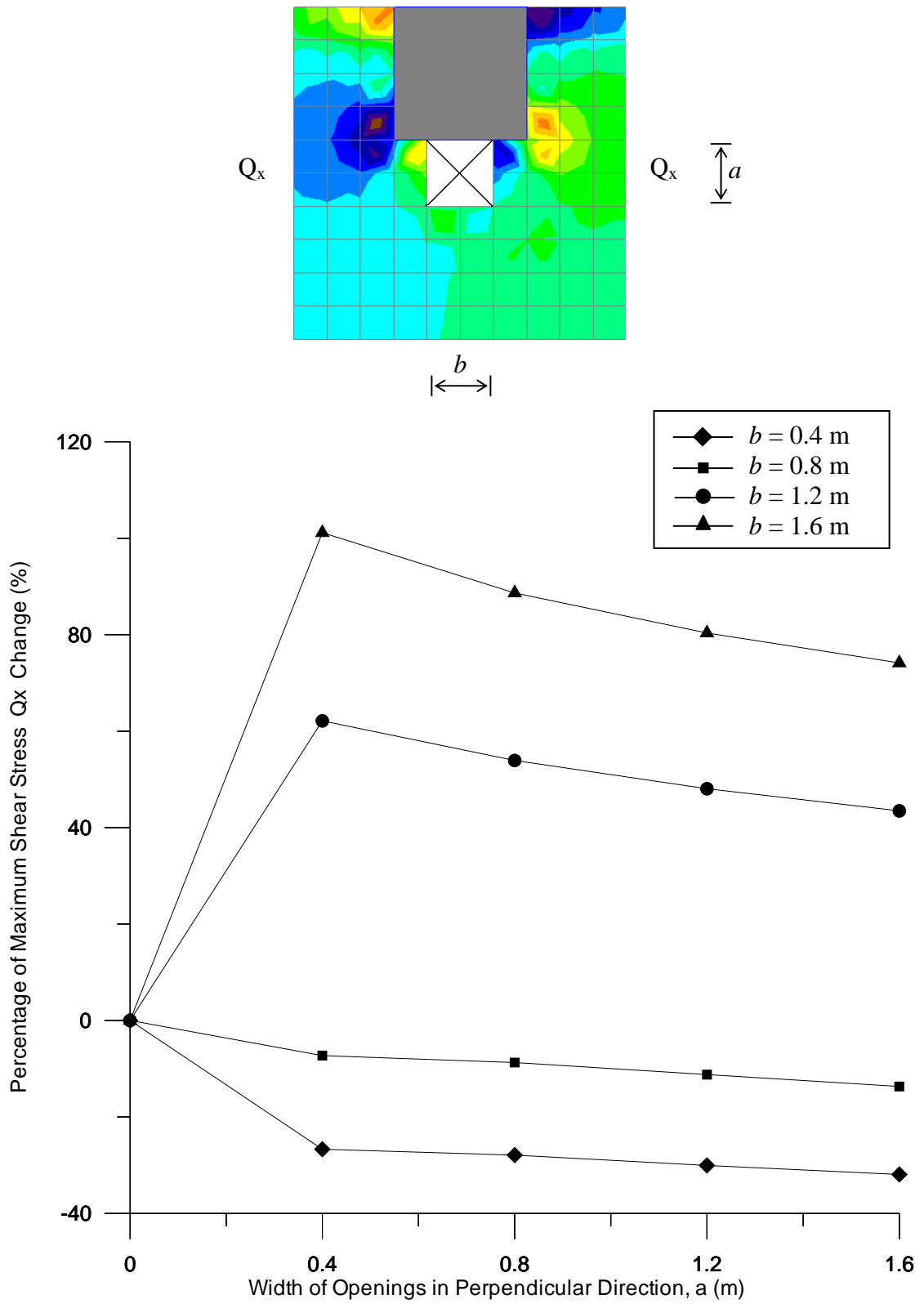


**Figure 51** Relationship between size of openings at “edge” and percentage of maximum shear stress  $Q_x$  change

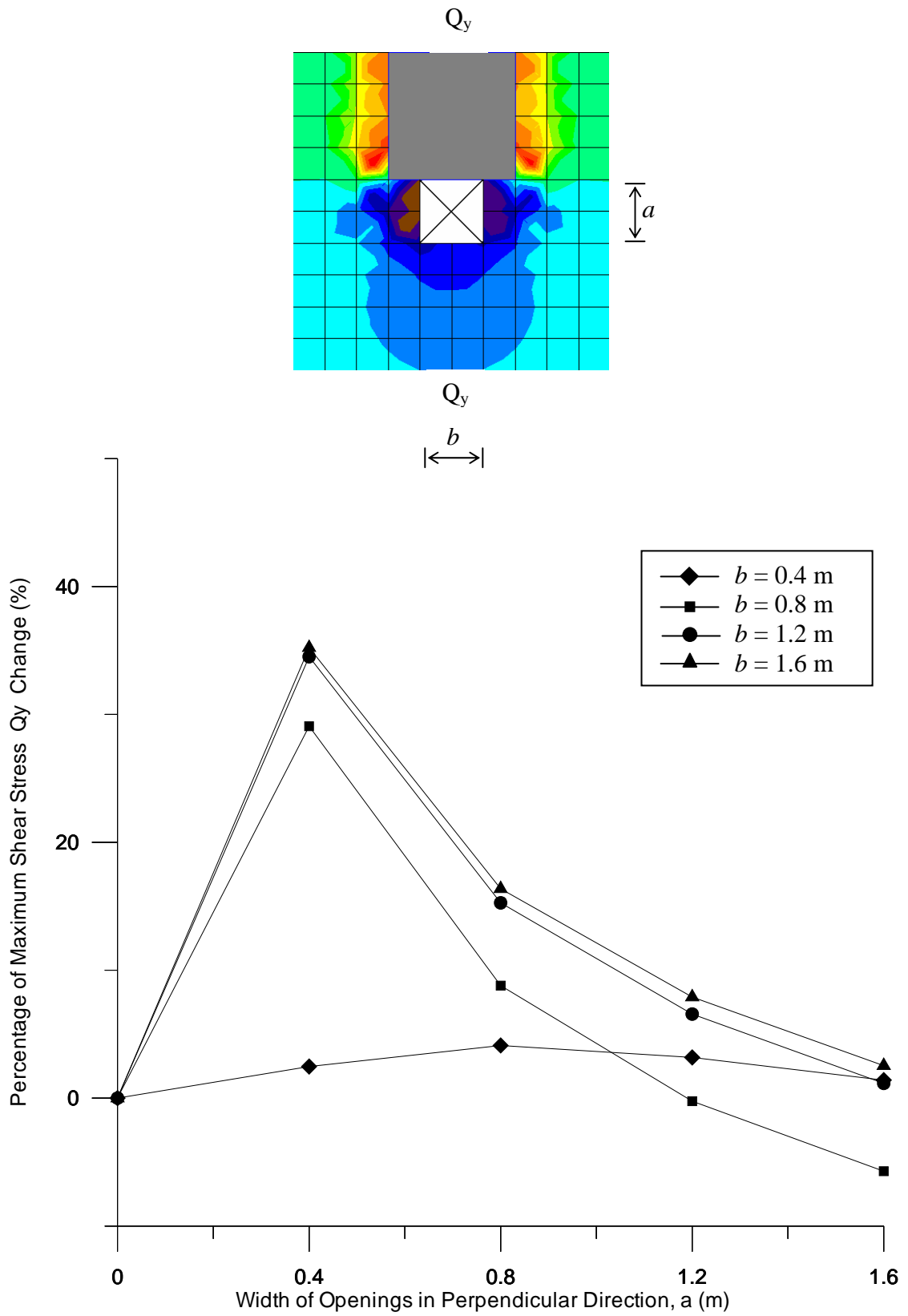


**Figure 52** Relationship between size of openings at “edge” and percentage of maximum shear stress  $Q_y$  change

In Figure 49, the percentage of maximum bending moment  $M_x$  is gradually reduced when the size of openings is expanded. It is reduced to 69.01% at the openings size  $a = 1.6$  m and  $b = 1.6$  m. The bending moment  $M_x$  in the area of column strip is always negative moment. When opening is expanded, the negative moment will be reduced and change to positive moment. The positive moment propagated from middle strip to column strip in the area of corner of openings adjacent the column is shown in Figures 53 to 56.

The percentage of maximum bending moment  $M_y$  change in Figure 50 will be reduced slightly -1.80% to -13.51% when the width of openings  $b = 0.4$  m where  $a$  varies from 0.4 m to 1.6 m respectively. But it is reduced rapidly to -45.05% when  $a = 0.4$  m and  $b = 1.6$  m. It is shown that the percentage of maximum bending moment  $M_y$  change rather constant when openings expanded in  $a$  direction but reduced rapidly when openings expanded in  $b$  direction. The maximum bending moment  $M_y$  concentrated at the corner of the opening as shown in Figure 57.

In Figure 51, the percentage of maximum shear stress  $Q_x$  change will be reduced when openings  $b = 0.4$  m and gradually reduced from -26.69% to -31.91% when  $a$  varies from 0.4 m to 1.6 m respectively. The percentage of maximum shear stress  $Q_x$  change will increase rapidly up to 101.14% when opening expanded in  $b$  direction at  $a = 0.4$  m and  $b = 1.6$  m. When sizes of openings expand larger, the percentage of maximum shear stress  $Q_x$  change will be reduced. Maximum shear stress  $Q_x$  concentrated at corner of column that is adjacent to the openings as shown in Figure 58.

The percentage of maximum shear stress  $Q_y$  illustrated in Figure 52, increases rapidly when the opening expands in parallel direction of the face of column. At size of opening  $a = 0.4$  m and  $b = 1.6$  m, percentage of maximum shear stress  $Q_y$  change increased equal to 35.22%. When sizes of openings expand larger, the percentage of maximum shear stress  $Q_y$  change will be reduced. Maximum shear stress  $Q_y$  concentrated at the corner of opening and propagated to the corner of column adjacent of the opening as shown in Figure 59.

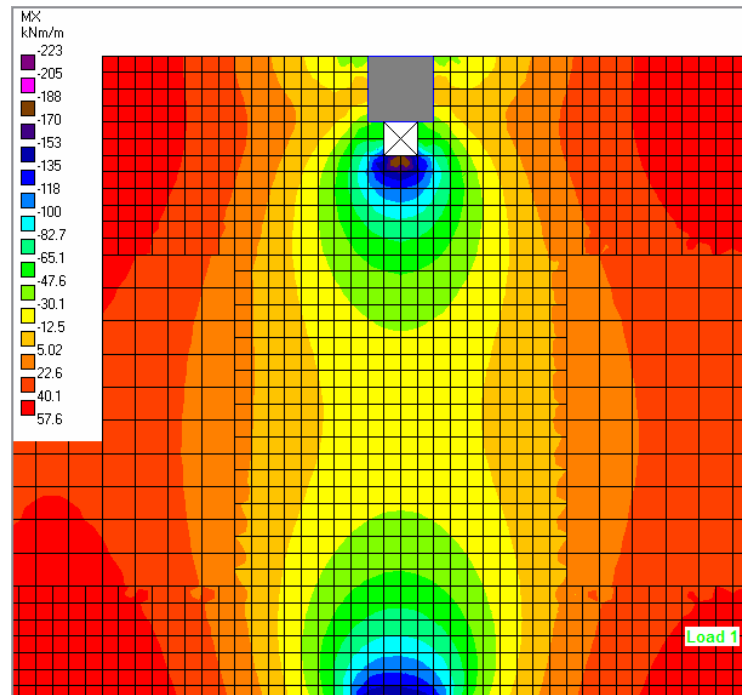


**Figure 53** Bending moment  $M_x$  concentration when opening  $a = 0.4$  m and  $b = 0.4$  m at “edge”

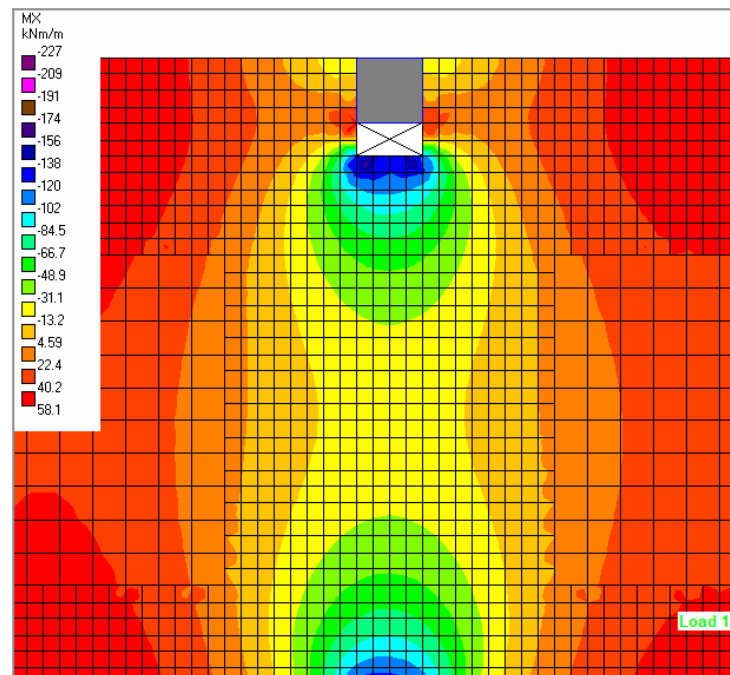


**Figure 54** Bending moment  $M_x$  concentration when opening  $a = 0.4$  m and  $b = 0.8$  m at “edge”

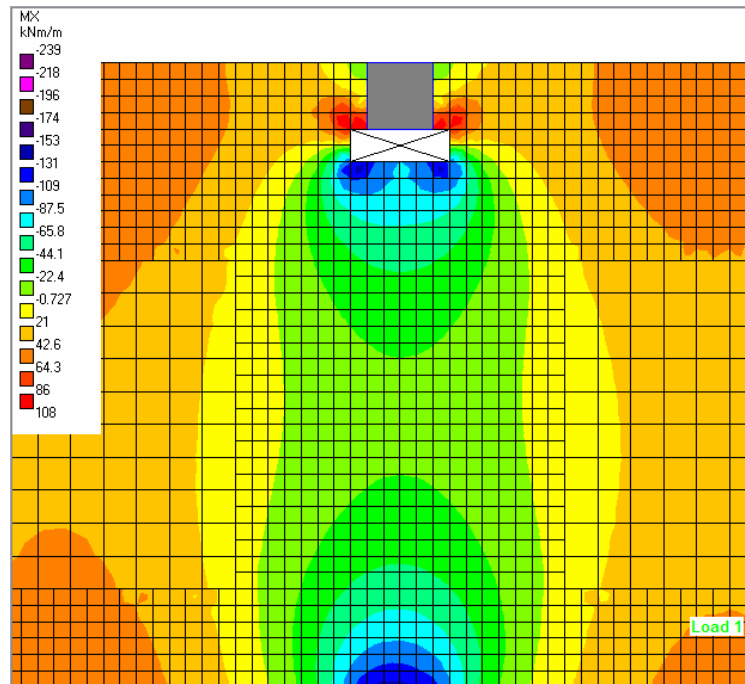


**Figure 55** Bending moment  $M_x$  concentration when opening  $a = 0.4$  m and  $b = 1.2$  m at “edge”

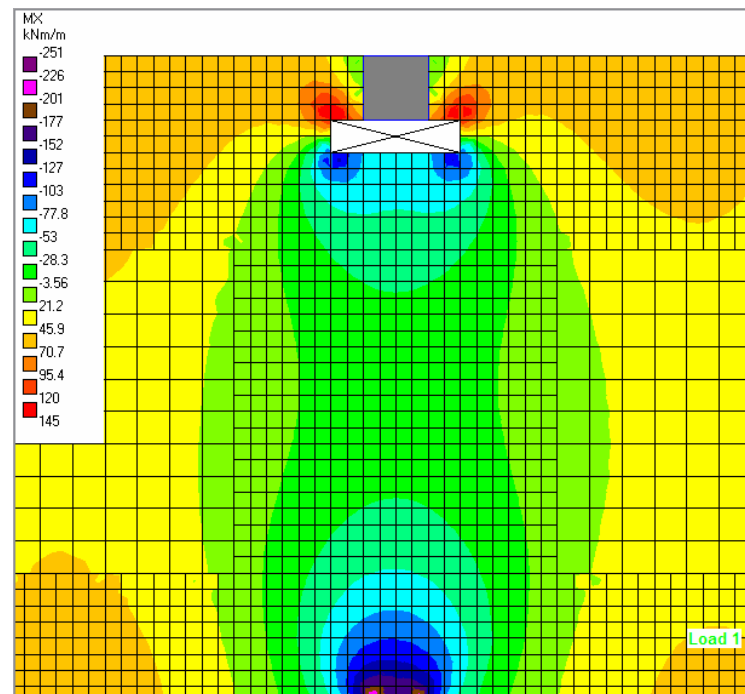


**Figure 56** Bending moment  $M_x$  concentration when opening  $a = 0.4$  m and  $b = 1.6$  m at “edge”

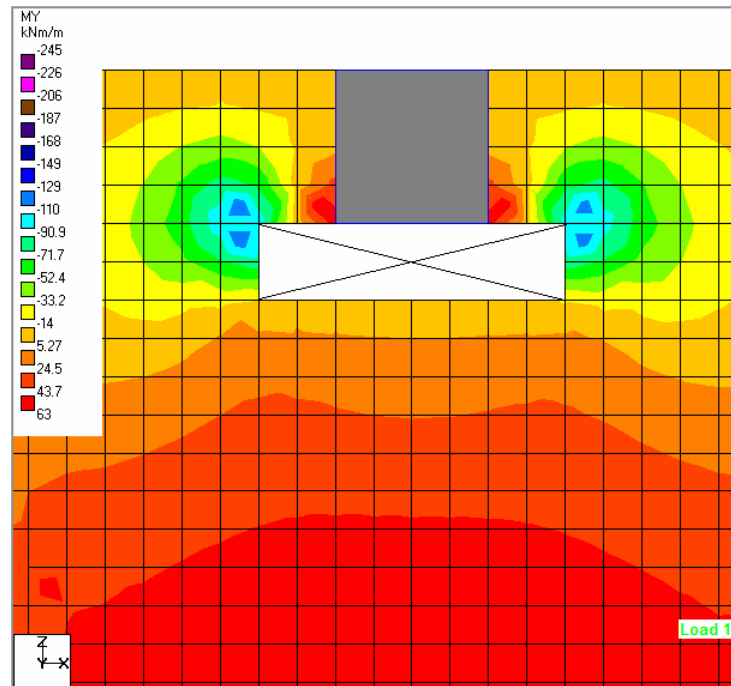


**Figure 57** Bending moment  $M_y$  concentration when opening  $a = 0.4$  m and  $b = 1.6$  m at “edge”

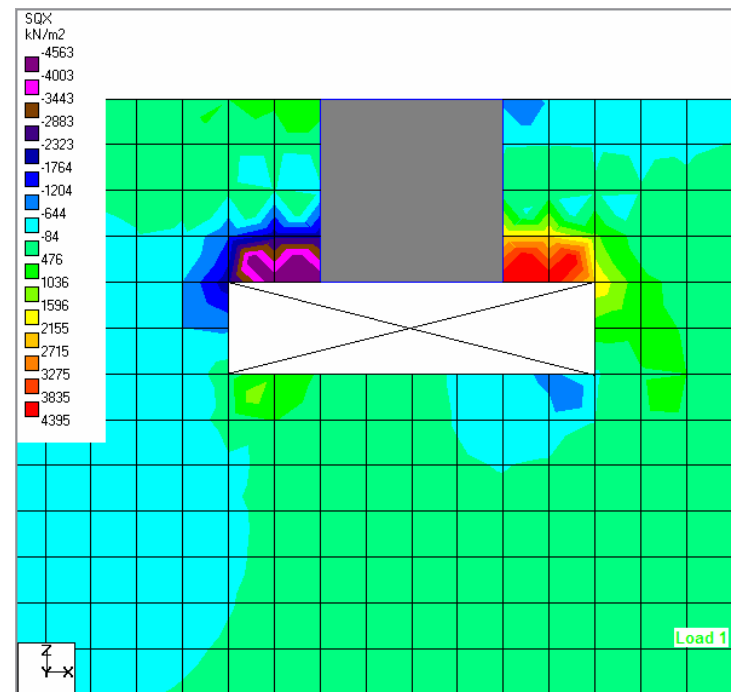


**Figure 58** Shear stress  $Q_x$  concentration when opening  $a = 0.4$  m and  $b = 1.6$  m at “edge”

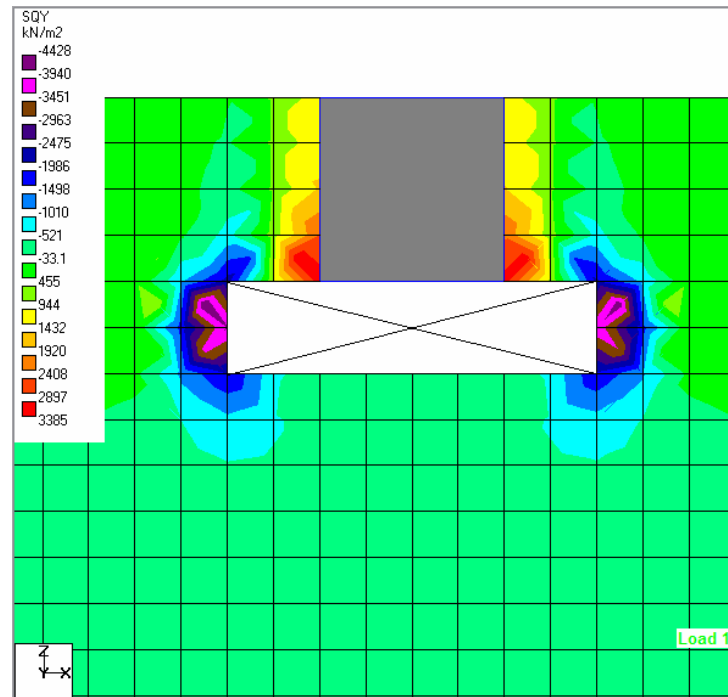


**Figure 59** Shear stress  $Q_y$  concentration when opening  $a = 0.4$  m and  $b = 1.6$  m at “edge”

From analysis the flat plates were classified into three categories with opening at the face of the column. At location “*in-in*” and “*in-ex*”, the critical size of openings is equal to  $a = 0.4$  m and  $b = 1.6$  m. The critical size of opening at the “*edge*” is equal to  $a = 0.4$  m and  $b = 1.6$  m too.

The location of maximum deflection “ $w$ ” of flat plate in  $z$ -direction without opening and opening at “*in-in*”, “*in-ex*”, and “*edge*” deflected in the same location that deflected in the area intersecting of middle strip of exterior panel. In Table 7, the maximum deflection “ $w$ ” of flat plate when opening  $a = 1.6$  m and  $b = 1.6$  m at location “*in-in*”, “*in-ex*”, and “*edge*” is close to the flat plate without opening.

**Table 7** Maximum deflection “ $w$ ” of flat plate in  $z$ -direction

maximum deflection “ $w$ ” (m)			
Without opening	Opening at “ <i>in-in</i> ”	Opening at “ <i>in-ex</i> ”	Opening at “ <i>edge</i> ”
0.0015	0.0016	0.0016	0.0017

**Table 8** Comparison of opening size and different location

Size ( $a \times b$ )  (m×m)	Change in $M_x$ (%)			Change in $M_y$ (%)			Change in $Q_x$ (%)			Change in $Q_y$ (%)		
	<i>“in-in”</i>	<i>“in-ex”</i>	<i>“edge”</i>									
0.4×0.4	3.23	1.38	-13.15	6.45	-3.69	-1.80	7.33	-7.90	-26.69	7.59	10.31	2.47
0.8×0.4	5.53	7.37	-22.07	11.98	-3.23	-6.31	14.26	-0.62	-27.93	14.56	8.36	4.12
1.2×0.4	7.37	11.52	-31.46	16.13	-1.84	-9.91	18.87	0.41	-30.06	19.28	11.33	3.18
1.6×0.4	8.29	14.29	-40.38	18.89	-0.46	-13.51	18.36	0.46	-31.91	22.56	14.62	1.41
0.4×0.8	5.99	7.37	-21.13	11.52	-2.76	-18.92	59.13	1.49	-7.29	16.31	74.21	29.08
0.8×0.8	8.29	12.90	-33.80	17.05	-0.46	-23.42	20.87	8.10	-8.71	22.67	34.82	8.80
1.2×0.8	9.22	16.59	-44.60	20.74	0.46	-26.58	24.72	12.05	-11.23	26.51	17.59	-0.24
1.6×0.8	10.14	18.89	-53.52	22.58	1.38	-29.28	27.23	14.72	-13.68	29.03	20.21	-5.71
0.4×1.2	11.98	17.97	-30.52	21.66	3.69	-29.28	67.69	59.23	62.12	35.03	81.82	34.51
0.8×1.2	12.90	22.12	-44.13	25.35	5.07	-30.18	33.69	36.56	53.91	38.31	46.15	15.27
1.2×1.2	13.36	24.42	-54.46	27.65	5.53	-32.43	34.51	27.49	48.05	40.15	29.64	6.57
1.6×1.2	13.28	25.81	-62.91	29.03	5.99	-34.68	35.85	28.72	43.46	41.33	29.85	1.16
0.4×1.6	14.29	27.65	-36.62	30.41	5.99	-45.05	71.59	46.31	101.14	48.31	83.44	35.22
0.8×1.6	14.75	29.95	-50.70	32.72	6.45	-44.59	41.79	38.05	88.63	49.59	50.97	16.37
1.2×1.6	14.75	31.34	-61.03	34.10	6.91	-45.95	42.82	38.62	80.35	50.15	37.54	7.91
1.6×1.6	14.75	31.80	-69.01	34.56	6.91	-46.85	43.28	38.87	74.13	50.41	38.00	2.54

3.2 Analyze the flat plates with openings at all edge columns that are represented by “*all-edge*” and all interior columns at exterior side that are represented by “*all-in*” as shown in Figures 60 and 61 respectively. Use the critical size of openings  $a = 0.4$  m and  $b = 1.6$  m. Determine percentage of maximum stress resultants change in area common to intersecting column strips A, B, C and D.

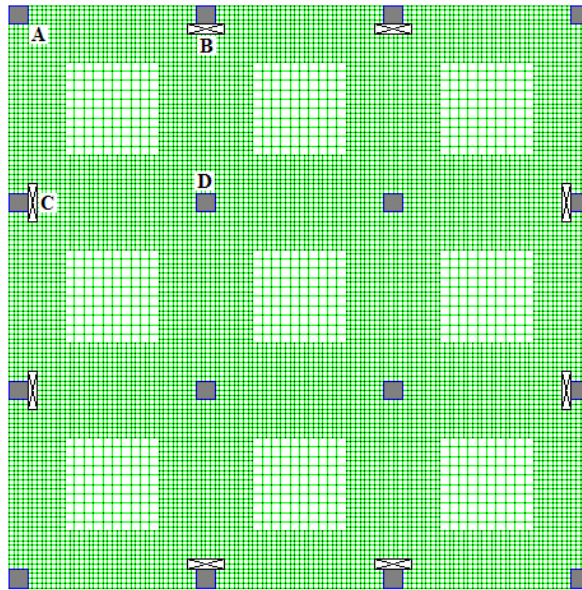


**Figure 60** Flat plate for opening critical size at “*all-edge*”

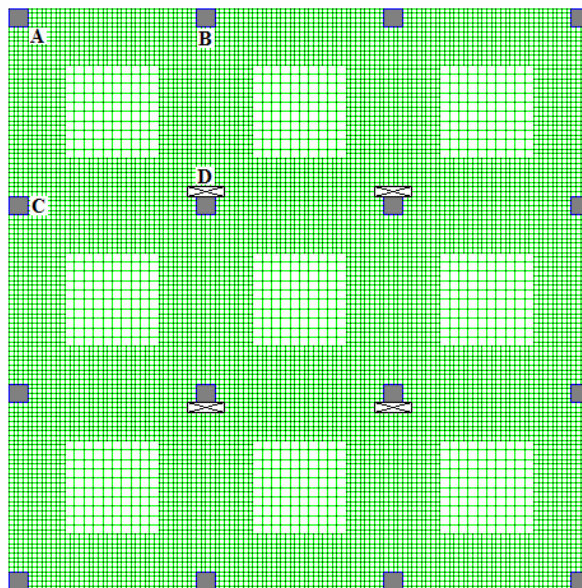


**Figure 61** Flat plate for opening critical size at “*all-in*”

**Table 9** Percentage of maximum bending moment  $M_x$  change of flat plate with opening at “*all-edge*” and “*all-in*”

Location	Percentage of maximum bending moment $M_x$ change (%)	
	“ <i>all-edge</i> ”	“ <i>all-in</i> ”
A	22.65	1.59
B	-29.16	5.23
C	-42.86	6.28
D	21.56	25.68

The bending moment  $M_x$  concentration in flat plate can be illustrated by Figure 62. In Table 9, when openings of flat plate are at “*all-edge*”, the percentage of maximum bending moment  $M_x$  change in area A and D are increased 22.65% and 21.56% respectively, while area B and C reduced 29.16% and 42.86% respectively. The bending moment  $M_x$  in area B is changed from negative to positive that propagates from middle strip as shown in Figure 63.

The openings at “*all-in*”, the percentage of maximum bending moment  $M_x$  change in area A, B, and C are increased slightly 1.59%, 5.23%, and 6.28% respectively. But in area D, it increased to 25.68% while positive moment propagated from middle strip to column strip as shown in Figure 64.

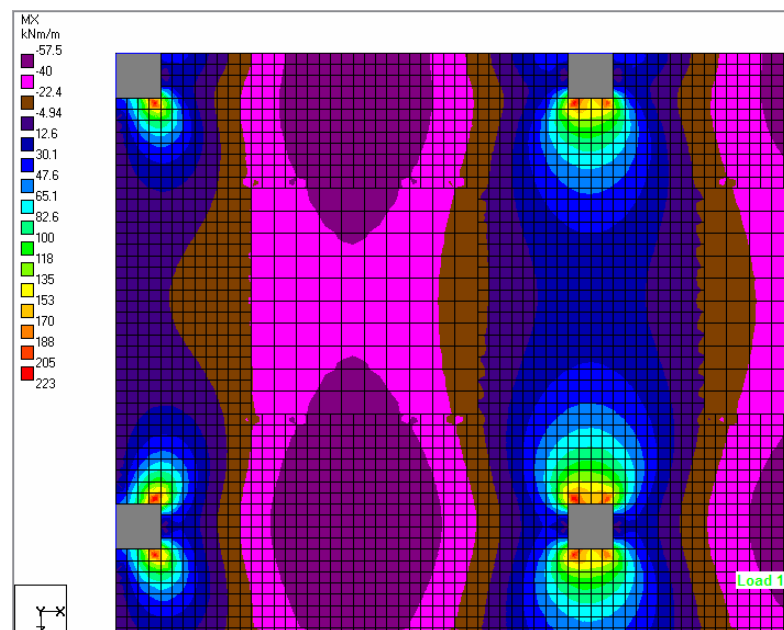


**Figure 62** Bending moment  $M_x$  concentration in flat plate

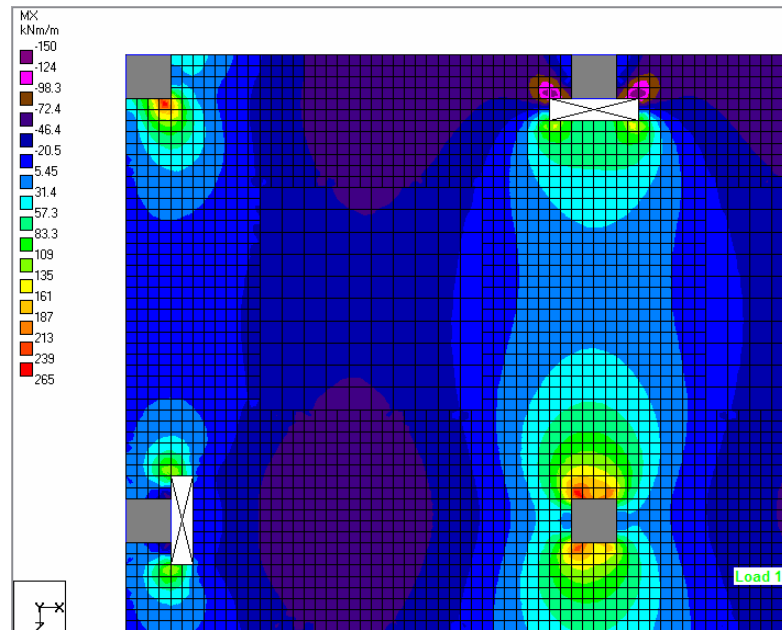


**Figure 63** Bending moment  $M_x$  concentration in flat plate with openings at “all-edge”

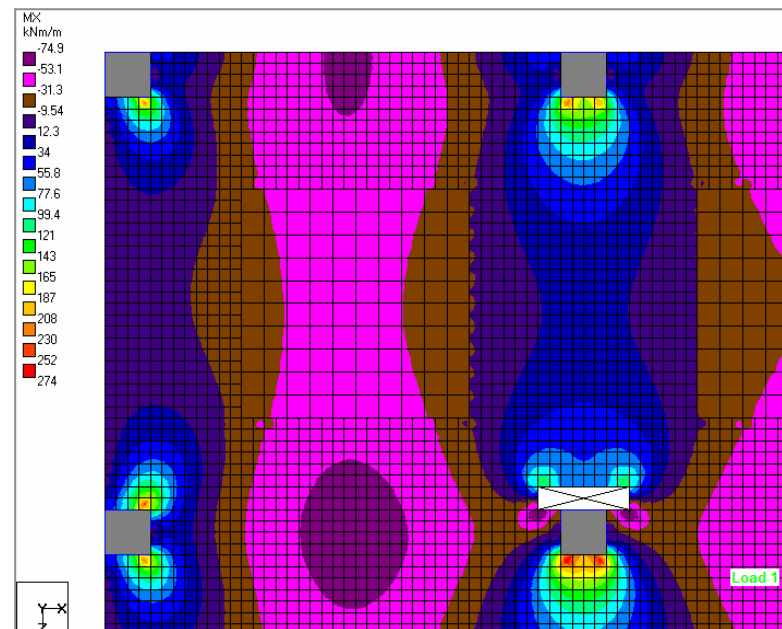


**Figure 64** Bending moment  $M_x$  concentration in flat plate with openings at “all-in”

**Table 10** Percentage of maximum bending moment  $M_y$  change of flat plate with opening at “*all-edge*” and “*all-in*”

Location	Percentage of maximum bending moment $M_y$ change (%)	
	“ <i>all-edge</i> ”	“ <i>all-in</i> ”
A	22.65	2.05
B	-42.86	11.42
C	-29.17	4.31
D	21.56	4.26

The bending moment  $M_y$  concentration in flat plate can be illustrated by Figure 65. In Table 10, when openings of flat plate are at “*all-edge*”, the percentage of maximum bending moment  $M_y$  change in area A and D are increased 22.65% and 21.56% respectively. While area B and C reduced 42.86% and 29.17% respectively. The bending moment  $M_y$  in area C is changed from negative to positive that propagates from middle strip as shown in Figure 66.

When the openings at “*all-in*” as shown in Figure 67, the percentage of maximum bending moment  $M_y$  change in area A, C, and D are increased slightly 2.05%, 4.31%, and 4.26% respectively. But in area B, it increased to 11.42%.

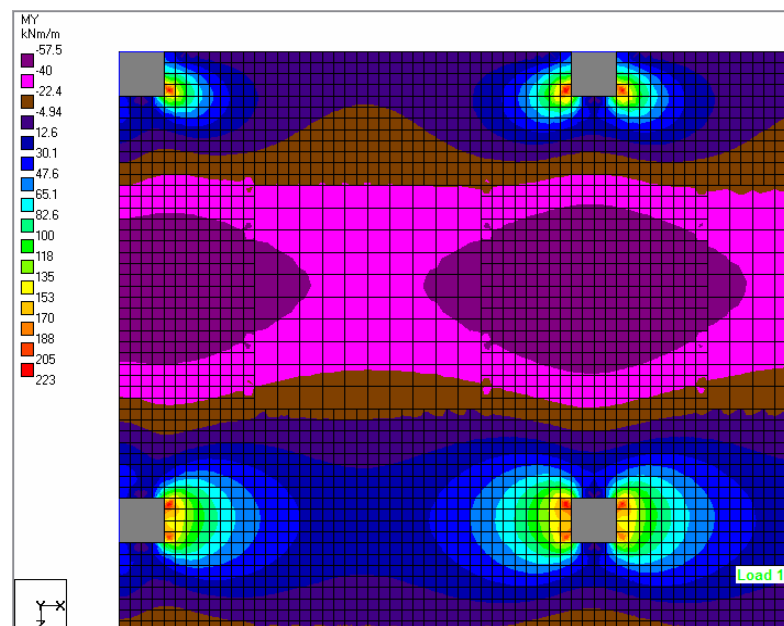


**Figure 65** Bending moment  $M_y$  concentration in flat plate

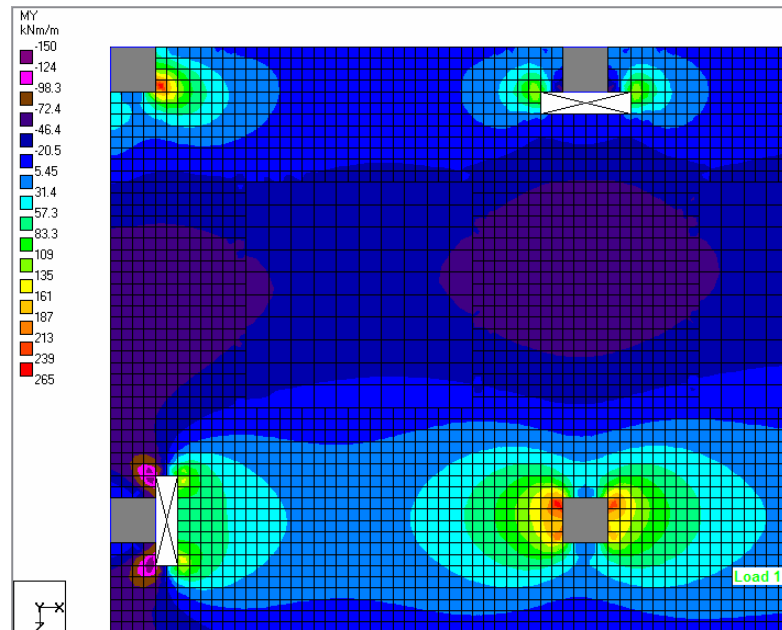


**Figure 66** Bending moment  $M_y$  concentration in flat plate with openings at “all-edge”

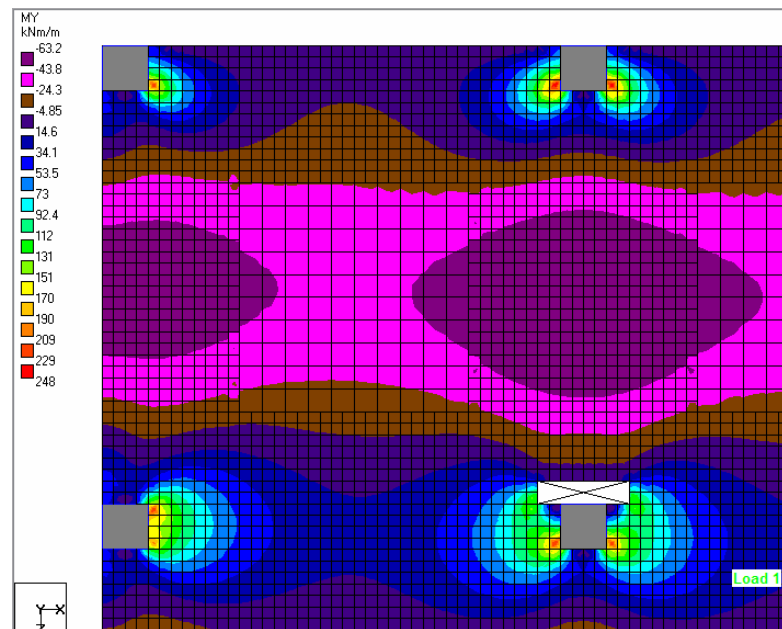


**Figure 67** Bending moment  $M_y$  concentration in flat plate with openings at “all-in”

**Table 11** Percentage of maximum shear stress  $Q_x$  change of flat plate with opening at “*all-edge*” and “*all-in*”

Location	Percentage of maximum shear stress $Q_x$ change (%)	
	“ <i>all-edge</i> ”	“ <i>all-in</i> ”
A	20.52	2.34
B	66.14	9.77
C	37.21	7.57
D	25.84	46.74

The shear stress  $Q_x$  concentration in flat plate can be illustrated by Figure 68. In Table 11, when openings of flat plate are at “*all-edge*”, the percentage of maximum shear stress  $Q_x$  change in area A, C, and D are increased 20.52%, 37.21% and 25.84% respectively. While area B increased to 66.14%. The shear stress  $Q_x$  concentrated in area of openings close to the corner of column as shown in Figure 69.

When openings at “*all-in*”, the percentage of maximum shear stress  $Q_x$  change in area A, B, and C are increased slightly 2.34%, 9.77%, and 7.57% respectively. But in area D, it increased to 46.74%. The shear stress  $Q_x$  concentrated in area of openings close to the corner of column as shown in Figure 70.

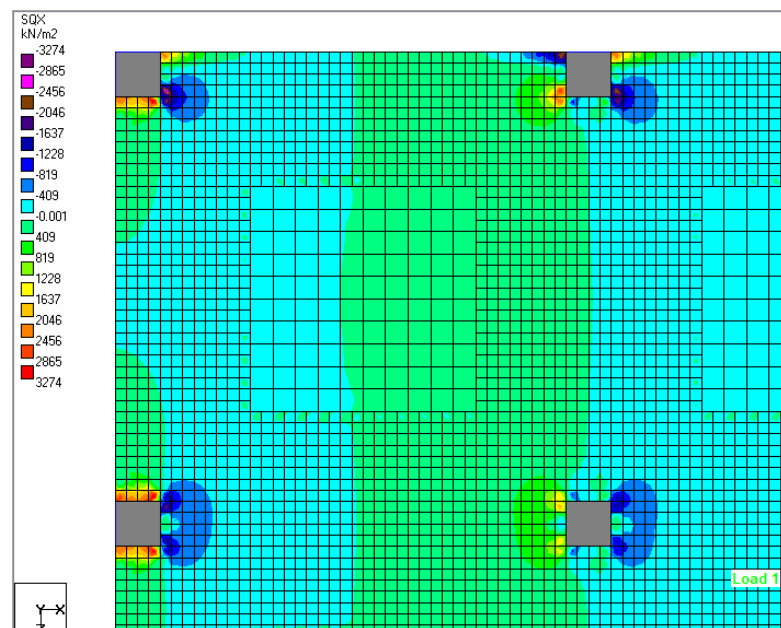


**Figure 68** Shear stress  $Q_x$  concentration in flat plate

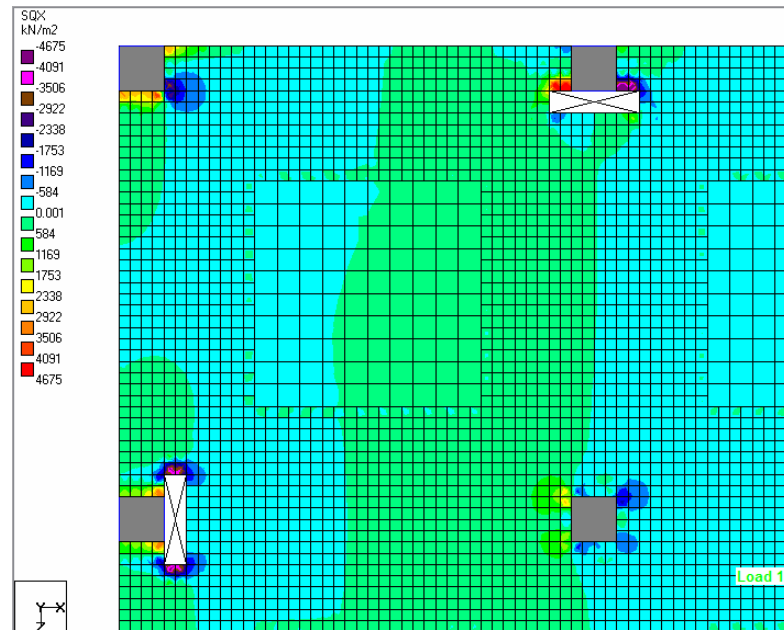


**Figure 69** Shear stress  $Q_x$  concentration in flat plate with openings at “all-edge”

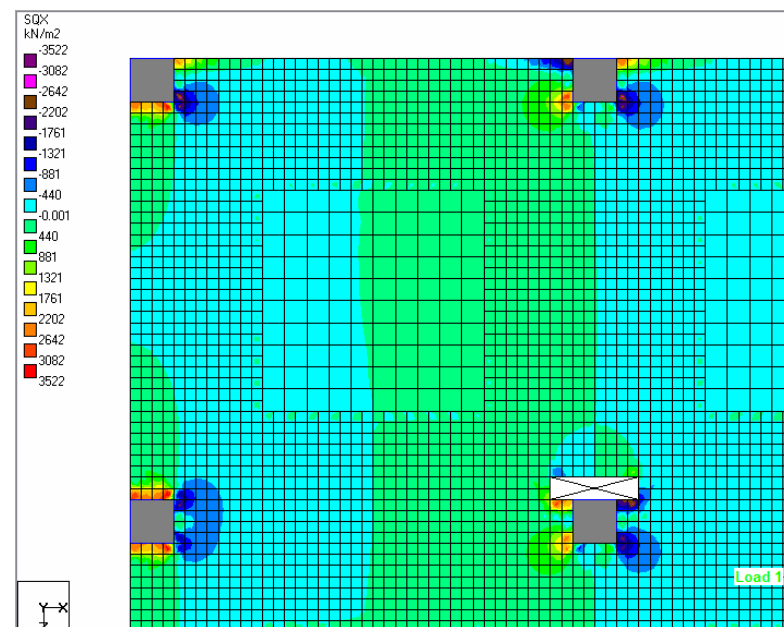


**Figure 70** Shear stress  $Q_x$  concentration in flat plate with openings at “all-in”

**Table 12** Percentage of maximum shear stress  $Q_y$  change of flat plate with opening at “*all-edge*” and “*all-in*”

Location	Percentage of maximum shear stress $Q_y$ change (%)	
	“ <i>all-edge</i> ”	“ <i>all-in</i> ”
A	20.52	3.29
B	37.21	13.17
C	66.14	6.23
D	25.84	83.75

The shear stress  $Q_y$  concentration in flat plate can be illustrated by Figure 71. In Table 12, when openings of flat plate are at “*all-edge*”, the percentage of maximum shear stress  $Q_y$  change in area A, B, and D are increased 20.52%, 37.21% and 25.84% respectively, while area C increased to 66.14%. The shear stress  $Q_y$  concentrated in area of openings close to the corner of column as shown in Figure 72.

When openings at “*all-in*”, the percentage of maximum shear stress  $Q_y$  change in area A, B, and C are increased slightly 3.29%, 13.17%, and 6.23% respectively. But in area D, it increased to 83.75%. The shear stress  $Q_y$  concentrated at corner of openings and propagated to the corner of column opposite side of opening as shown in Figure 73.

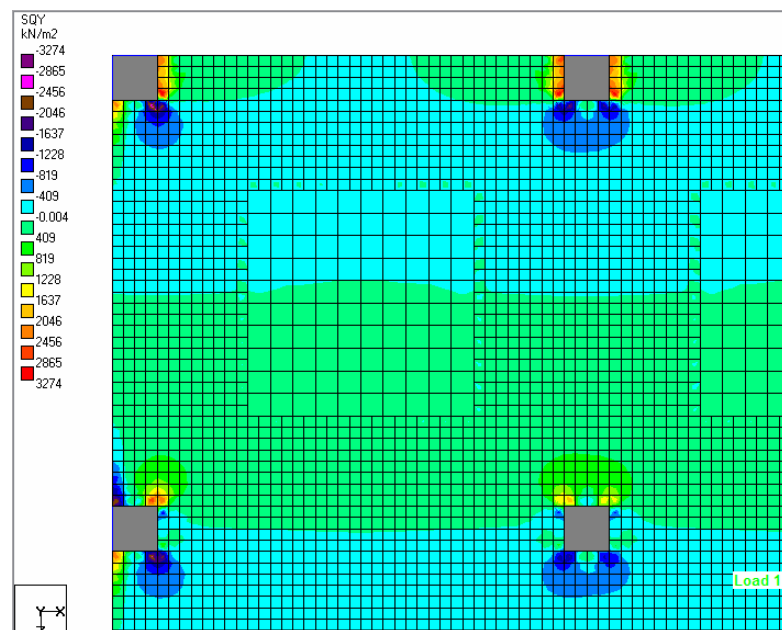


**Figure 71** Shear stress  $Q_y$  concentration in flat plate

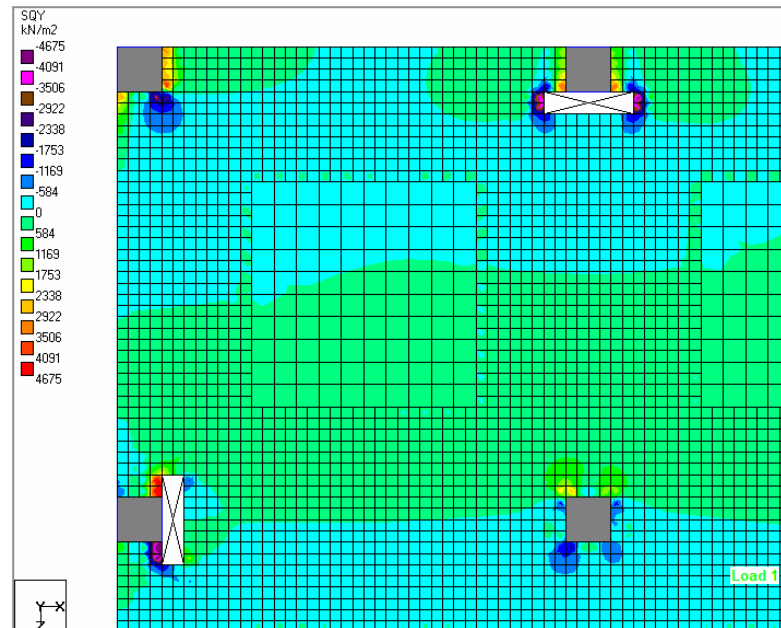


**Figure 72** Shear stress  $Q_y$  concentration in flat plate with openings at "all-edge"

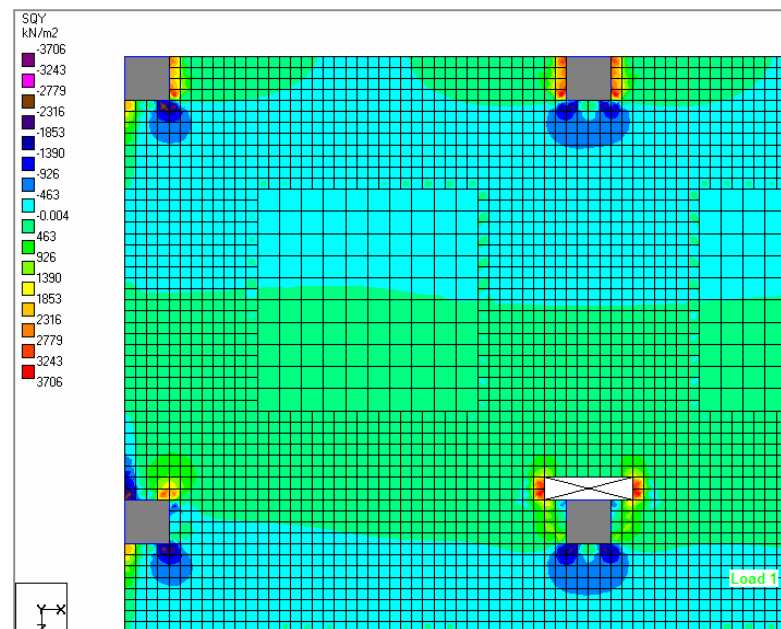


**Figure 73** Shear stress  $Q_y$  concentration in flat plate with openings at "all-in"

## CONCLUSION

The main results of the behavior of flat plate with large openings in column strip by analysis with program *STAAD.Pro* are summarized as follows.

1. In column strip, the openings at the face of the column are more critical than the openings at the corner of column. The shear stress at the edge column is greater than the interior column so should avoid opening of flat plate in the area of the face of the edge column.

2. With the openings at interior column and interior side, the sizes of opening affect the stress resultants when the openings expand in parallel direction of the face of the column. When the width  $b$  of opening is equal to 1.6 m the percentage of stress resultants change are increased. The bending moment  $M_x$  is increased and flat out at 14.75%, the bending moment  $M_y$  increased to 34.56%, shear stress  $Q_x$  increased rapidly to 71.59%, and shear stress  $Q_y$  increased and flat out at 50.41%.

3. With the openings at interior column and exterior side, the sizes of opening affect the stress resultants when the openings expand in parallel direction of the face of the column. When the width  $b$  of opening is equal to 1.6 m the percentage of bending moment  $M_x$  increased to 31.80%, the bending moment  $M_y$  increased slightly to 6.91%, shear stress  $Q_x$  increased rapidly to 83.44%, and shear stress  $Q_y$  increased to 46.31%.

4. With the openings at edge column, the bending moment was reduced when the openings expanded and change direction of bending from negative to positive. When the opening is equal to 1.6 m the percentage of bending moment  $M_x$  is reduced to 69.01%, and  $M_y$  reduced to 46.85%, shear stress  $Q_x$  increased to 101.14%, and shear stress  $Q_y$  increased to 35.22%.

5. With the openings at all edge columns by  $a = 0.4$  m and  $b = 1.6$  m, the bending moment at corner and interior column were increased 22.65% and 21.56% respectively but at edge column it reduced to 42.86%. For shear stress, at corner and interior column were increased 20.52% and 25.84% respectively but at edge column it increased to 66.14%.

6. With the openings at all interior columns by  $a = 0.4$  m and  $b = 1.6$  m, the bending moment at corner column increased 2.05%, at interior column it increased 25.68% and at edge column it increased 11.42%. For shear stress, at corner column it increased 3.29%, at edge column it increased 13.17% and at interior column it increased 83.75%.

## **RECOMMENDATION**

Recommendation for further research can be summarized as follows.

1. The openings in column strip of flat plate caused the increase of bending moment. Further study should be done on how to place flexural reinforcement to resist the increasing bending moment while spacing of reinforcement is narrow.
2. Shear stress increase can be prevented by using drop panel and shear stud. Further study should be carried out about the method used for drop panel and shear stud. In case of edge column, edge beam can be used to resist the shear stress.
3. Further research should be carried out about pattern load that affects the stress resultants in flat plate.

## LITERATURE CITED

- ACI Committee 318. 1995. **Building Code Requirements for Structural Concrete (ACI 318M-95) and Commentary-ACI 318RM-95**. American Concrete Institute, Detroit.
- Cook, R.D., D.S. Malkus, M.E. Plesha and R.J. Witt. 2002. **Concepts and Applications of Finite Element Analysis**. 4<sup>th</sup> ed. John Wiley&Sons, Inc., New York.
- E.I.T. Committee. 1973. **Reinforce Concrete building Code by Ultimate Strength**. 1<sup>st</sup> ed. Bangkok.
- Ghosh, S.K. and B.G. Rabbat. 1990. **Building Code Requirements for Reinforce Concrete (ACI318-89)**. 5<sup>th</sup> ed. Portland Cement Association, Illinois.
- Nilson, A.H. 1997. **Design of Concrete Structures**. 12<sup>th</sup> ed. McGraw-Hill, Singapore.
- Prawat, R. 2000. **Study of Behavior of Flat Plates with Large Opening**. M.S. Thesis, Kasetsart University.
- Research Engineers International. 2002. **STAAD.Pro 2002 Technical Reference Manual**. Division of netGuru, Singapore.
- Salakawy E.F. 1998. Investigating The Behavior of Reinforced Concrete Flat Slabs with Opening. **In Concrete Abstracts of American Concrete Institute**. Faemington Hills, United States of America. P388.
- Timoshenko, S.P. and S. Woinowsky-Krieger. 1959. **Theory of Plates and Shells**. 2<sup>nd</sup> ed. McGraw-Hill, Singapore.
- Wang, C.K. and C.G. Salmon. 1992. **Reinforced Concrete Design**. 5<sup>th</sup> ed. HarperCollinsDaniel Publisher, Inc., New York.